TABLE 1. HISTOMORPHOMETRY OF TRABECULAR BONE OF LUMBAR VERTEBRAE

	BV/TV (%)	Ob.S/BS (%)	MAR (μm/day)	BFR (μm³/μm²/day)	N.Oc/B.Pm (/100 mm)	Oc.S/BS (%)	ES/BS (%)
Male							
WT	16.48 ± 2.09	6.27 ± 0.63	0.94 ± 0.19	0.08 ± 0.02	94.24 ± 11.31	2.10 ± 0.15	3.45 ± 0.49
SRC-1$^{-/-}$	11.53 ± 1.39*	9.15 ± 0.81*	1.40 ± 0.15*	0.13 ± 0.02	159.05 ± 12.02†	3.50 ± 0.21†	5.73 ± 0.57†
Female							
WT	12.97 ± 0.65	8.55 ± 0.51	1.02 ± 0.11	0.11 ± 0.01	109.66 ± 12.64	2.41 ± 0.19	3.72 ± 0.25
SRC-1$^{-/-}$	7.73 ± 0.95†	11.02 ± 1.32	1.42 ± 0.08*	0.18 ± 0.03*	174.95 ± 24.39*	4.28 ± 0.31†	6.47 ± 0.21†

Parameters for the trabecular bone were measured in an area 0.3 mm in length from cortical bone at the fifth lumbar vertebrae in toluidine blue and calcein double-labeled sections. Data are expressed as means ± SEM (n = 15/group for males and n = 12/group for females). BV/TV, trabecular bone volume expressed as a percentage of total tissue volume; Ob.S/BS, percentage of bone surface covered by cuboidal osteoblasts; MAR, mineral apposition rate; BFR, bone formation rate expressed by MAR × percentage of bone surface exhibiting double labels plus one half single labels; N.Oc/B.Pm, number of mature osteoclasts in 10 cm of bone perimeter; Oc.S/BS, percentage of bone surface covered by mature osteoclasts; ES/BS, percentage of eroded surface.
*$p < 0.05$; †$p < .01$; significantly different from WT mice.

TABLE 2. SERUM AND URINARY BIOCHEMISTRY

	Serum							Urine
	ALP (IU/liter)	Osteocalcin (ng/ml)	Ca (mg/dl)	P (mg/dl)	Leptin (ng/ml)	Testosterone (ng/ml)	17β-estradiol (pg/ml)	DPD (nM/mM Cr)
Male								
WT	78.16 ± 6.91	20.61 ± 1.76	7.93 ± 0.21	7.52 ± 0.49	6.01 ± 0.74	2.45 ± 0.33	2.34 ± 0.21	8.29 ± 0.42
SRC-1$^{-/-}$	99.67 ± 8.16*	26.42 ± 2.16*	8.11 ± 0.18*	7.51 ± 0.57	7.45 ± 0.57	3.41 ± 0.42*	2.78 ± 0.28	11.31 ± 0.1†
Female								
WT	90.22 ± 5.74	25.05 ± 1.62	8.04 ± 0.11	7.18 ± 0.29	6.87 ± 0.67	ND	5.18 ± 0.57	9.32 ± 0.19
SRC-1$^{-/-}$	117.13 ± 7.72*	33.34 ± 1.41†	7.87 ± 0.19	7.15 ± 0.41	8.18 ± 1.24	ND	7.12 ± 0.64*	12.71 ± 0.28†

Data are expressed as means ± SEM (n = 15/group for males and n = 12/group for females). *ALP*, alkaline phosphatase; *Ca*, calcium; *P*, phosphorus; *DPD*, deoxypyridinoline; ND, not detected.
Concentration of *DPD* was collected according to urinary creatinine concentration.
*$p < 0.05$; †$p < 0.01$; significantly different from WT mice.

sex hormone levels through a feedback mechanism becomes too weak to catch up with the decreased sensitivity to these hormones by the SRC-1 deficiency.

Administration experiments with steroid hormones revealed that the SRC-1 deficiency caused resistance to osteoanabolic actions of sex hormones in gonadectomized male and female mice. More interesting is that *SRC-1*$^{-/-}$ mice exhibited osteopenia under physiological conditions at 24 weeks, suggesting a bone-sparing role of endogenous SRC-1. This is also likely to be caused by the impairment of actions of endogenous sex hormones on bone for the following reasons. First, morphological and biochemical analyses revealed that *SRC-1*$^{-/-}$ mice exhibited the decrease in trabecular bone with a high turnover state, which is characteristic of the pathology of sex hormone deficiencies. Second, the serum sex hormone levels were upregulated in *SRC-1*$^{-/-}$ mice of both sexes, implicating a compensatory reaction for the insensitivity to them. Third, in the absence of sex hormones by gonadectomies, the BMD decreased to similar levels between WT and *SRC-1*$^{-/-}$ mice. These results indicate that the SRC-1 function is essential for the maintenance of bone mass by sex hormones under both physiological and pathological conditions.

In males, as well as activating the AR, androgens can be converted into estrogens by the enzyme aromatase,[30] and therefore can exert their effects not only through the AR, but also through the ERs. Because DHT cannot be converted to estrogens by aromatase, loss of the osteoanabolic effect of exogenous DHT in *SRC-1*$^{-/-}$ orchidectomized male mice can be interpreted as a defect in AR, but not ER, signaling. Furthermore, we and others recently revealed that the androgen/AR signaling is indispensable for male-type bone remodeling, independent of the estrogen/ER signaling, by the analysis of AR-deficient mice.[31,32] Under physiological conditions, however, there are many reports showing the essential contribution of the estrogen/ER signaling to male bones. Inhibition of aromatase activity in male rats impairs bone remodeling and mimics the effect of orchidectomy,[33,34] and the aromatase-deficient mice develop osteopenia.[35] Two men with mutations in the *aromatase P450* gene exhibited delayed skeletal maturation and osteopenia, despite high levels of circulating androgens and the ability to respond to estradiol.[36,37] These observations are similar to those seen in a man with a mutation in the ER,[38] reinforcing the importance of the estrogen/ER signaling in male bones. In addition, the SRC-1 transcriptional activation of AR is known to be much weaker than that of ERs.[39] Therefore, the bone loss seen in *SRC-1*$^{-/-}$ males may, at least in part, be caused by impairment of the

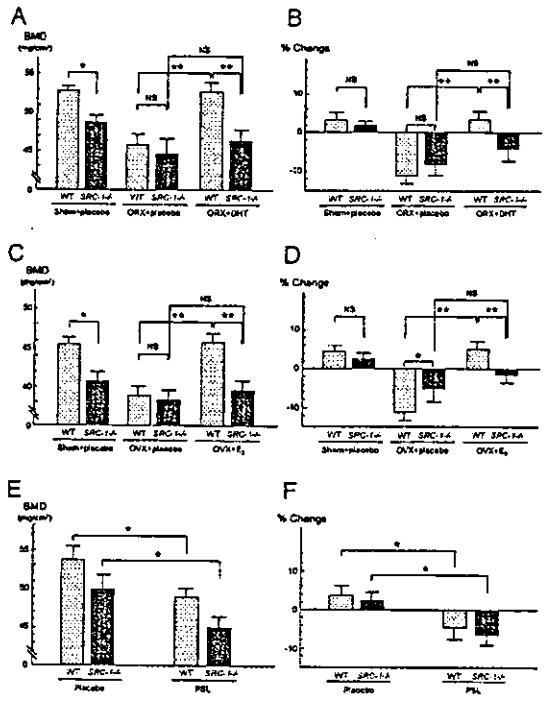

FIG. 4. Effects of gonadectomy and hormone administrations on BMD of vertebrae in *SRC-1*$^{-/-}$ and WT littermates. (A and B) Male WT and *SRC-1*$^{-/-}$ littermates were orchidectomized or sham-operated at 16 weeks of age and implanted subcutaneously with slow-releasing pellets containing either placebo or DHT (10 mg/pellet). At 16 and 24 weeks of age, BMD of the fifth lumbar vertebrae was measured by DXA. (C and D) Female WT and *SRC-1*$^{-/-}$ littermates were ovariectomized or sham-operated at 16 weeks of age and implanted subcutaneously with slow-releasing pellets containing either placebo or E_2 (0.025 mg/pellet). BMD was measured as described above. (E and F) Male WT and *SRC-1*$^{-/-}$ littermates without operation were implanted subcutaneously with slow-releasing pellets containing either placebo or prednisolone (PSL; 4 mg/pellet) at 16 weeks of age. BMD was measured as described above. Both the (A, C, and E) raw BMD values of the excised vertebrae at 24 weeks and (B, D, and F) the percent changes of BMD of the vertebrae measured in situ during 8 weeks were compared between WT and *SRC-1*$^{-/-}$ mice. Data in all graphs are expressed as means (bars) ± SE (error bars) for 8 mice/group. Significant difference: $*p < 0.05$, $**p < 0.01$. NS, not significant ($p > 0.05$).

estrogen/ER signaling, as well as of the androgen/AR signaling.

It is interesting that SRC-1 deficiency caused the decrease of trabecular bone but not of cortical bone. Similar findings are reported in a study using the conventional *SRC-1* knockout mice.[29] A previous study examining ERα and ERβ expressions by immunohistochemistry in neonatal human ribs showed that trabecular bone contains both ERs, whereas only ERα was detected in cortical bone.[40] Modder et al.[29] also showed that the cancellous bone of the mouse vertebrae contains both ERs, whereas the cortical bone of the mouse femur contains exclusively ERα. In addition, another recent study revealed that, in osteoblastic cells, SRC-1 potentiates the transcriptional activity of co-expressed ERα/ERβ or ERβ alone, with little or no potentiation of ERα.[41] Hence, as Modder et al.[29] stated in their report, at least in females, the discrepancy of the SRC-1 contribution between trabecular and cortical bone may be caused by the relative expression of ERα versus ERβ in the two kinds of bone and to the specific interactions of SRC-1 with these receptor isoforms in bone cells. In males as well, difference of effects on the two kinds of bone can be explained by the distinctions of expression and activation of the ER isoforms, because estrogen/ER signaling is important in male bone, as described above. Regarding AR, its distribution in the trabecular and cortical bones remains unknown. Further studies on the expression and the interaction with SRC-1 of AR and ERs will elucidate the clinical importance of SRC-1 in human bones.

The conventional *SRC-1* knockout mice are reported to be obesity prone under a high-fat diet.[42] In this study as well, our *SRC-1*$^{-/-}$ mice, fed a standard diet, showed higher body weight and serum leptin levels compared with those of WT littermates, although both were slight and not statistically significant. A series of recent reports showed that leptin, an anorexigenic hormone secreted by adipocytes, also shows antiosteogenic action centrally through hypothalamic and sympathetic nervous systems.[43] However, this low level of increase in the leptin level seems inadequate to explain the significant bone loss by the SRC-1 deficiency. In addition, the *SRC-1*$^{-/-}$ bone exhibited high bone turnover with stimulated bone formation, which is the opposite of leptin action.

Nuclear receptors exert their tissue-specific function using different coactivator/corepressor complexes ingeniously and appropriately in each tissue.[11,12,44] Therefore, it is possible that not only the dysfunction of nuclear receptors or their ligands, but also that of the cofactors, leads to various disorders. The function of cofactors might explain the difference among individuals in the sensitivity to hormones and related agents as well. Despite important roles of sex hormones in bone, the effect of their gain or loss of function varies widely among individuals, and this has not yet been fully explained by analyses of the receptor levels. Accumulated genetic studies have failed to identify a definite association of the ER or AR gene polymorphisms with BMD.[45] Furthermore, a case of testicular feminization in a patient without an AR gene mutation was reported as a possible co-factor disease.[46] From the results of this study, SRC-1 may be a strong candidate that regulates the variety of the pathophysiology of sex hormone-deficient osteoporosis and therapeutic effects of hormone replacements in humans, because humans are known to be more sensitive to sex hormone deficiency than mice.

ACKNOWLEDGMENTS

We thank Dr Yasuji Yamamoto (Taiho Pharmaceutical Co., Ltd.) for helpful discussion and Kaori Yamamoto (ELK Corp.) and the hard tissue research team at Kureha Chemical Industry Co., Ltd. for technical assistance. This study was supported by a Grant-in-Aid for Scientific Research from the Japanese Ministry of Education, Culture, Sports, Science, and Technology (15659348).

TABLE 3. EFFECTS OF GONADECTOMIES AND HORMONE REPLACEMENTS ON REPRODUCTIVE TISSUES

	WT			*SRC-1*$^{-/-}$		
	Sham + placebo	*Gonadectomy + placebo*	*Gonadectomy + hormone*	*Sham + placebo*	*Gonadectomy + placebo*	*Gonadectomy + hormone*
Seminal vesicle weights of males (g)	0.31 ± 0.03	0.03 ± 0.01*	0.35 ± 0.03	0.28 ± 0.03	0.03 ± 0.01*	0.18 ± 0.02†
Uterine weights of females (g)	0.12 ± 0.02	0.02 ± 0.01*	0.13 ± 0.03	0.11 ± 0.03	0.02 ± 0.01*	0.05 ± 0.02†

Data are expressed as means ± SEM (n = 8/group for males and females).
*$p < 0.01$, significantly different from the respective sham group.
†$p < 0.01$, significantly different from the respective WT mice.

TABLE 4. COMPARISON BETWEEN TWO *SRC-1*$^{-/-}$ KNOCKOUT MICE

	Modder et al.[29]	*This study*
Generation of mice		
Targeting method	Conventional	Floxed mice × CMV-Cre transgenic mice
Locus of stop codon	Exon 11	Exon 5
Genetic background	C57BL/6	C57BL/6
Physiological conditions		
Age of analysis	12 weeks	12 & 24 weeks
Skeletal phenotype		
12 weeks	Normal	Normal
24 weeks	—	Osteopenia
Hormone administration experiments		
Age	12–20 weeks	16–24 weeks
Estrogen action on females	Decreased	Decreased
Estrogen dose/pellet	15 μg/60-d & 60 μg/60-d	25 μg/60-d
Androgen action on males	—	Decreased
Glucocorticoid action on males	—	Unaffected

REFERENCES

1. Evans RM 1988 The steroid and thyroid hormone receptor superfamily. Science 240:889–895.
2. Mangelsdorf DJ, Thummel C, Beato M, Herrlich P, Schutz G, Umesono K, Blumberg B, Kastner P, Mark M, Chambon P, Evans RM 1995 The nuclear receptor superfamily: The second decade. Cell 83:835–839.
3. Tsai MJ, O'Malley BW 1994 Molecular mechanisms of action of steroid/thyroid receptor superfamily members. Annu Rev Biochem 63:451–486.
4. Bland R 2000 Steroid hormone receptor expression and action in bone. Clin Sci (Lond) 98:217–240.
5. Compston JE 2001 Sex steroids and bone. Physiol Rev 81:419–447.
6. Bilezikian JP 2002 Sex steroids, mice, and men: When androgens and estrogens get very close to each other. J Bone Miner Res 17:563–566.
7. Riggs BL, Khosla S, Melton LJ III 2002 Sex steroids and the construction and conservation of the adult skeleton. Endocr Rev 23:279–302.
8. Francis RM 1999 The effects of testosterone on osteoporosis in men. Clin Endocrinol (Oxf) 50:411–414.
9. Canalis E 1996 Clinical review 83: Mechanisms of glucocorticoid action in bone. Implications to glucocorticoid-induced osteoporosis. J Clin Endocrinol Metab 81:3441–3447.
10. Osella G, Terzolo M, Reimondo G, Piovesan A, Pia A, Termine A, Paccotti P, Angeli A 1997 Serum markers of bone and collagen turnover in patients with Cushing's syndrome and in subjects with adrenal incidentalomas. J Clin Endocrinol Metab 82:3303–3307.
11. Glass CK, Rosenfeld MG 2000 The coregulator exchange in transcriptional functions of nuclear receptors. Genes Dev 14:121–141.
12. McKenna NJ, O'Malley BW 2002 Combinatorial control of gene expression by nuclear receptors and coregulators. Cell 108:465–474.
13. Xu J, O'Malley BW 2002 Molecular mechanisms and cellular biology of the steroid receptor coactivator (SRC) family in steroid receptor function. Rev Endocr Metab Disord 3:185–192.
14. Onate SA, Tsai SY, Tsai MJ, O'Malley BW 1995 Sequence and characterization of a coactivator for the steroid hormone receptor superfamily. Science 270:1354–1357.
15. Hong H, Kohli K, Trivedi A, Johnson DL, Stallcup MR 1996 GRIP1, a novel mouse protein that serves as a transcriptional coactivator in yeast for the hormone binding domains of steroid receptors. Proc Natl Acad Sci USA 93:4948–4952.
16. Voegel JJ, Heine MJ, Zechel C, Chambon P, Gronemeyer H 1996 TIF2, a 160 kDa transcriptional mediator for the ligand-dependent activation function AF-2 of nuclear receptors. EMBO J 15:3667–3675.
17. Carapeti M, Aguiar RC, Watmore AE, Goldman JM, Cross NC 1999 Consistent fusion of MOZ and TIF2 in AML with inv(8)(p11q13). Cancer Genet Cytogenet 113:70–72.
18. Bautista S, Valles H, Walker RL, Anzick S, Zeillinger R, Meltzer P, Theillet C 1998 In breast cancer, amplification of the steroid receptor coactivator gene AIB1 is correlated with estrogen and progesterone receptor positivity. Clin Cancer Res 4:2925–2929.
19. Ghadimi BM, Schrock E, Walker RL, Wangsa D, Jauho A, Meltzer PS, Ried T 1999 Specific chromosomal aberrations and amplification of the AIB1 nuclear receptor coactivator gene in pancreatic carcinomas. Am J Pathol 154:525–536.
20. Xu J, Qiu Y, DeMayo FJ, Tsai SY, Tsai MJ, O'Malley BW 1998 Partial hormone resistance in mice with disruption of the steroid receptor coactivator-1 (SRC-1) gene. Science 279:1922–1925.
21. Weiss RE, Xu J, Ning G, Pohlenz J, O'Malley BW, Refetoff S 1999 Mice deficient in the steroid receptor co-activator 1 (SRC-1) are resistant to thyroid hormone. EMBO J 18:1900–1904.
22. Weiss RE, Gehin M, Xu J, Sadow PM, O'Malley BW, Chambon P, Refetoff S 2002 Thyroid function in mice with compound heterozygous and homozygous disruptions of SRC-1 and TIF-2

coactivators: Evidence for haploinsufficiency. Endocrinology 143: 1554–1557.
23. Takeuchi Y, Murata Y, Sadow P, Hayashi Y, Seo H, Xu J, O'Malley BW, Weiss RE, Refetoff S 2002 Steroid receptor coactivator-1 deficiency causes variable alterations in the modulation of T(3)-regulated transcription of genes in vivo. Endocrinology 143:1346–1352.
24. Nakamichi Y, Shukunami C, Yamada T, Aihara K, Kawano H, Sato T, Nishizaki Y, Yamamoto Y, Shindo M, Yoshimura K, Nakamura T, Takahashi N, Kawaguchi H, Hiraki Y, Kato S 2003 Chondromodulin I is a bone remodeling factor. Mol Cell Biol 23:636–644.
25. Ferretti JL 2000 Peripheral Quantitative Computed Tomography for Evaluating Structural and Mechanical Properties of Small Bone Mechanical Testing of Bone and the Bone-Implant Interface. CRC Press, Boca Raton, FL, USA, pp. 385–405.
26. Parfitt AM, Drezner MK, Glorieux FH, Kanis JA, Malluche H, Meunier PJ, Ott SM, Recker RR 1987 Bone histomorphometry: Standardization of nomenclature, symbols, and units. Report of the ASBMR Histomorphometry Nomenclature Committee. J Bone Miner Res 2:595–610.
27. Heery DM, Kalkhoven E, Hoare S, Parker MG 1997 A signature motif in transcriptional co-activators mediates binding to nuclear receptors. Nature 387:733–736.
28. Spencer TE, Jenster G, Burcin MM, Allis CD, Zhou J, Mizzen CA, McKenna NJ, Onate SA, Tsai SY, Tsai MJ, O'Malley BW 1997 Steroid receptor coactivator-1 is a histone acetyltransferase. Nature 389:194–198.
29. Modder UI, Sanyal A, Kearns AE, Sibonga JD, Nishihara E, Xu J, O'Malley BW, Ritman EL, Riggs BL, Spelsberg TC, Khosla S 2004 Effects of loss of steroid receptor coactivator-1 on the skeletal response to estrogen in mice. Endocrinology 145:913–921.
30. Simpson ER, Mahendroo MS, Means GD, Kilgore MW, Hinshelwood MM, Graham-Lorence S, Amarneh B, Ito Y, Fisher CR, Michael MD, Mendelson CR, Bulun SE 1994 Aromatase cytochrome P450, the enzyme responsible for estrogen biosynthesis. Endocr Rev 15:342–355.
31. Yeh S, Tsai MY, Xu Q, Mu XM, Lardy H, Huang KE, Lin H, Yeh SD, Altuwaijri S, Zhou X, Xing L, Boyce BF, Hung MC, Zhang S, Gan L, Chang C 2002 Generation and characterization of androgen receptor knockout (ARKO) mice: An in vivo model for the study of androgen functions in selective tissues. Proc Natl Acad Sci USA 99:13498–13503.
32. Kawano H, Sato T, Yamada T, Matsumoto T, Sekine K, Watanabe T, Nakamura T, Fukuda T, Yoshimura K, Yoshizawa T, Aihara K, Yamamoto Y, Nakamichi Y, Metzger D, Chambon P, Nakamura K, Kawaguchi H, Kato S 2003 Suppressive function of androgen receptor in bone resorption. Proc Natl Acad Sci USA 100:9416–9421.
33. Vanderschueren D, Van Herck E, De Coster R, Bouillon R 1996 Aromatization of androgens is important for skeletal maintenance of aged male rats. Calcif Tissue Int 59:179–183.
34. Vanderschueren D, van Herck E, Nijs J, Ederveen AG, De Coster R, Bouillon R 1997 Aromatase inhibition impairs skeletal modeling and decreases bone mineral density in growing male rats. Endocrinology 138:2301–2307.
35. Oz OK, Zerwekh JE, Fisher C, Graves K, Nanu L, Millsaps R, Simpson ER 2000 Bone has a sexually dimorphic response to aromatose deficiency. J Bone Miner Res 15:507–514.
36. Morishima A, Grumbach MM, Simpson ER, Fisher C, Qin K 1995 Aromatase deficiency in male and female siblings caused by a novel mutation and the physiological role of estrogens. J Clin Endocrinol Metab 80:3689–3698.
37. Carani C, Qin K, Simoni M, Faustini-Fustini M, Serpente S, Boyd J, Korach KS, Simpson ER 1997 Effect of testosterone and estradiol in a man with aromatase deficiency. N Engl J Med 337:91–95.
38. Smith EP, Boyd J, Frank GR, Takahashi H, Cohen RM, Specker B, Williams TC, Lubahn DB, Korach KS 1994 Estrogen resistance caused by a mutation in the estrogen-receptor gene in a man. N Engl J Med 331:1056–1061.
39. Auger AP, Tetel MJ, McCarthy MM 2000 Steroid receptor coactivator-1 (SRC-1) mediates the development of sex-specific brain morphology and behavior. Proc Natl Acad Sci USA 97: 7551–7555.
40. Bord S, Horner A, Beavan S, Compston J 2001 Estrogen receptors alpha and beta are differentially expressed in developing human bone. J Clin Endocrinol Metab 86:2309–2314.
41. Monroe DG, Johnsen SA, Subramaniam M, Getz BJ, Khosla S, Riggs BL, Spelsberg TC 2003 Mutual antagonism of estrogen receptors alpha and beta and their preferred interactions with steroid receptor coactivators in human osteoblastic cell lines. J Endocrinol 176:349–357.
42. Picard F, Gehin M, Annicotte J, Rocchi S, Champy MF, O'Malley BW, Chambon P, Auwerx J 2002 SRC-1 and TIF2 control energy balance between white and brown adipose tissues. Cell 111:931–941.
43. Takeda S, Karsenty G 2001 Central control of bone formation. J Bone Miner Metab 19:195–198.
44. Yanagisawa J, Kitagawa H, Yanagida M, Wada O, Ogawa S, Nakagomi M, Oishi H, Yamamoto Y, Nagasawa H, McMahon SB, Cole MD, Tora L, Takahashi N, Kato S 2002 Nuclear receptor function requires a TFTC-type histone acetyl transferase complex. Mol Cell 9:553–562.
45. Liu YZ, Liu YJ, Recker RR, Deng HW 2003 Molecular studies of identification of genes for osteoporosis: The 2002 update. J Endocrinol 177:147–196.
46. Adachi M, Takayanagi R, Tomura A, Imasaki K, Kato S, Goto K, Yanase T, Ikuyama S, Nawata H 2000 Androgen-insensitivity syndrome as a possible coactivator disease. N Engl J Med 343: 856–862.

Address reprint requests to:
Hiroshi Kawaguchi, MD, PhD
Department of Orthopaedic Surgery
Faculty of Medicine
University of Tokyo
Hongo 7-3-1, Bunkyo
Tokyo 113-8655, Japan
E-mail: kawaguchi-ort@h.u-tokyo.ac.jp

Received in original form December 19, 2003; in revised form April 14, 2004; accepted May 7, 2004.

THE JOURNAL OF BIOLOGICAL CHEMISTRY

Vol. 279, No. 32, Issue of August 6, pp. 33684–33695, 2004
Printed in U.S.A.

Reduced Pain Hypersensitivity and Inflammation in Mice Lacking Microsomal Prostaglandin E Synthase-1*

Received for publication, January 8, 2004, and in revised form, April 22, 2004
Published, JBC Papers in Press, May 12, 2004, DOI 10.1074/jbc.M400199200

Daisuke Kamei‡§, Kiyofumi Yamakawa§¶, Yui Takegoshi‡, Maya Mikami-Nakanishi‡, Yoshihito Nakatani‡, Sachiko Oh-ishi‡, Hidekazu Yasui‖, Yoshiaki Azuma‖, Noriyasu Hirasawa, Kazuo Ohuchi**, Hiroshi Kawaguchi¶, Yukio Ishikawa‡‡, Toshiharu Ishii‡‡, Satoshi Uematsu§§, Shizuo Akira§§, Makoto Murakami‡, and Ichiro Kudo‡¶¶**

*From the ‡Department of Health Chemistry, School of Pharmaceutical Sciences, Showa University, 1-5-8 Hatanodai, Shinagawa-ku, Tokyo 142-8555, the ¶Department of Orthopedic Surgery, Faculty of Medicine, University of Tokyo, 7-3-1 Hongo, Bunkyo-ku, Tokyo 113-8655, ‖Pharmaceutical Discovery Research Laboratories, the Institute for Biomedical Research, Teijin Pharma Limited, 4-3-2 Asahigaoka, Hino-shi, Tokyo 191-8512, the **Laboratory of Pathophysiological Biochemistry, Graduate School of Pharmaceutical Sciences, Tohoku University, Aoba Aramaki, Aoba-ku, Sendai, Miyagi 980-8578, the ‡‡Department of Pathology, Toho University, School of Medicine, 5-21-16 Omori-Nishi, Ohta-ku, Tokyo 143-8540, and the §§Department of Host Defense, Research Institute for Microbial Diseases, Osaka University, 3-1 Yamada-oka, Suita, Osaka 565-0871, Japan*

We examined the *in vivo* role of membrane-bound prostaglandin E synthase (mPGES)-1, a terminal enzyme in the PGE_2-biosynthetic pathway, using mPGES-1 knockout (KO) mice. Comparison of PGES activity in the membrane fraction of tissues from mPGES-1 KO and wild-type (WT) mice indicated that mPGES-1 accounted for the majority of lipopolysaccharide (LPS)-inducible PGES in WT mice. LPS-stimulated production of PGE_2, but not other PGs, was impaired markedly in mPGES-1-null macrophages, although a low level of cyclooxygenase-2-dependent PGE_2 production still remained. Pain nociception, as assessed by the acetic acid writhing response, was reduced significantly in KO mice relative to WT mice. This phenotype was particularly evident when these mice were primed with LPS, where the stretching behavior and the peritoneal PGE_2 level of KO mice were far less than those of WT mice. Formation of inflammatory granulation tissue and attendant angiogenesis in the dorsum induced by subcutaneous implantation of a cotton thread were reduced significantly in KO mice compared with WT mice. Moreover, collagen antibody-induced arthritis, a model for human rheumatoid arthritis, was milder in KO mice than in WT mice. Collectively, our present results provide unequivocal evidence that mPGES-1 contributes to the formation of PGE_2 involved in pain hypersensitivity and inflammation.

Prostaglandin (PG)[1] E_2 is the most common prostanoid, being produced by a variety of cells and tissues, and has a broad range of biological activity. Recent advances in this research field have led to molecular identification and characterization of various enzymes involved in the biosynthesis of PGE_2, including phospholipase A_2 (PLA_2), cyclooxygenase (COX) and terminal PGE synthase (PGES) (1). Each of these three enzymatic steps can be rate limiting for PGE_2 biosynthesis and involves multiple enzymes/isozymes that can act in different phases of cell activation. The PGE_2 produced thus far is then released from the cells and acts on the four types of PGE receptor, EP1, EP2, EP3, and EP4, which are coupled with trimeric G protein signaling (2).

PGES, which catalyzes the conversion of PGH_2 to PGE_2, exists as membrane-associated and cytosolic enzymes. Two of them are membrane-bound enzymes and have been designated as mPGES-1 and mPGES-2 (3–16). mPGES-1 is a glutathione (GSH)-requiring perinuclear protein belonging to the MAPEG (for membrane-associated proteins involved in eicosanoid and GSH metabolism) family (4–6). This enzyme is induced markedly by proinflammatory stimuli, is down-regulated by anti-inflammatory glucocorticoids, and is functionally coupled with COX-2 in marked preference to COX-1. Induction of mPGES-1 expression has also been observed in various systems in which COX-2-derived PGE_2 has been implicated to play a critical role, such as inflammation, fever, pain, female reproduction, tissue repair, and cancer (4–12). Inducible expression of mPGES-1 is in part regulated by the mitogen-activated protein kinase pathways (13), where the kinases may switch on the inducible transcription factor Egr-1 that in turn binds to the proximal GC box in the *mPGES-1* promoter, leading to mPGES-1 transcription (14). mPGES-2, which has a catalytic glutaredoxin- or thioredoxin-like domain and is activated by various thiol reagents, is synthesized as a Golgi membrane-associated protein, and the proteolytic removal of the N-terminal hydrophobic domain leads to the formation of a mature cytosolic enzyme (15, 16). This enzyme is rather constitutively expressed in various cells and tissues and is functionally coupled with both COX-1 and COX-2 (16). Cytosolic PGES (cPGES), a GSH-requiring enzyme constitutively expressed in a wide variety of cells, is functionally linked to COX-1, not COX-2, to promote immediate PGE_2 production (17). This enzyme is regulated by formation of a complex with Hsp90, a molecular chaperone (18). In addition, two cytosolic GSH-*S*-transferases (μ2 and μ3) have the ability to catalyze the isomerization of PGH_2 to PGE_2, at least *in vitro* (19).

* This work was supported by grants-in aid for scientific research from the Ministry of Education, Science, Culture, Sports, and Technology of Japan. The costs of publication of this article were defrayed in part by the payment of page charges. This article must therefore be hereby marked "*advertisement*" in accordance with 18 U.S.C. Section 1734 solely to indicate this fact.

§ These authors equally contributed to this work.

¶¶ To whom correspondence should be addressed. Tel.: 81-3-3784-8196; Fax: 81-3-3784-8245; E-mail: kudo@pharm.showa-u.ac.jp.

[1] The abbreviations used are: PG, prostaglandin; BMD, bone mineral density; CAIA, collagen antibody-induced arthritis; CIA, collagen-induced arthritis; COX, cyclooxygenase; cPGES, cytosolic PGES; $cPLA_2\alpha$, cytosolic phospholipase $A_2\alpha$; HDC, histidine decarboxylase; KO, knockout; LPS, lipopolysaccharide; mPGES, membrane-bound PGES; PGES, PGE synthase; siRNA, small interfering RNA; TBS, Tris-buffered saline; TRAP, tartrate-resistant acid phosphatase; VEGF, vascular endothelial cell growth factor; WT, wild-type.

The importance of PGE_2 in various pathophysiological events dictates the necessity to understand the role of each PGES enzyme *in vivo*. In fact, biochemical and cell biological analyses have led to the proposal that among the PGES enzymes identified so far, mPGES-1 may be most critically responsible for the production of the PGE_2 implicated in various pathophysiological events. An initial study with mPGES-1 knock-out (KO) mice has reported the essential role of mPGES-1 in lipopolysaccharide (LPS)-stimulated delayed PGE_2 production by macrophages, although these mice are fertile, develop normally after birth, and retain LPS-stimulated production of various cytokines (20). In this study, we used mPGES-1 KO mice to analyze the role of mPGES-1 in inflammation-associated pain hypersensitivity, tissue granulation accompanying angiogenesis, and arthritis induced by collagen antibody.

EXPERIMENTAL PROCEDURES

Animals—Male C57BL/6 mice were obtained from Saitama Animal Center. The mPGES-1 KO mice and littermate wild-type (WT) mice (C57BL/6 × 129/SvJ background) were described previously (20). Male mice (7 weeks old) were used in each experiment. Mice were housed in microisolator cages in a pathogen-free barrier facility, and all experiments were performed under approved institutional guidance.

Agents—LPS (*Escherichia coli* 0111:B4), goat anti-mouse vascular endothelial cell growth factor (VEGF), and indomethacin were purchased from Sigma. Mouse anti-human $cPLA_2\alpha$ monoclonal antibody and goat anti-human COX-1 and COX-2 polyclonal antibodies were purchased from Santa Cruz Biotechnology. Rabbit antibodies against human mPGES-1 (12), mPGES-2 (16), and cPGES (17) were prepared as described previously. Rabbit anti-mouse histidine decarboxylase (HDC) antibody was donated by Dr. S. Tanaka (Kyoto University) (21). Enzyme immunoassay kits for PGE_2, 6-keto-$PGF_{1\alpha}$ (a stable end product of PGI_2), $PGF_{2\alpha}$, and thromboxane B_2 (a stable end product of thromboxane A_2) and the COX-2 inhibitor NS-398 were purchased from Cayman Chemicals. The COX-1 inhibitor valeryl salicylate was a generous gift from Dr. W. Smith (University of Michigan). Oligonucleotides were purchased from Bex.

Measurement of PGES Activity—PGES activity was measured by assessment of conversion of PGH_2 to PGE_2 as reported previously (4). Briefly, cell or tissue homogenates were centrifuged at 100,000 × *g* for 1 h at 4 °C, and the membrane fractions were used as an enzyme source. An aliquot (10 μg of protein equivalents) was incubated with 0.5 μg of PGH_2 for 30 s at 24 °C in 0.1 ml of 0.1 M Tris-HCl (pH 8.0) containing 1 mM glutathione and 5 μg of indomethacin. After stopping the reaction by the addition of 100 mM $FeCl_2$, the PGE_2 content of the reaction mixture was quantified by use of the enzyme immunoassay kit.

Preparation and Activation of Peritoneal Macrophages—Peritoneal cells were recovered from mice that had received thioglycollate medium (Difco) (1 ml/20 g of body weight) 4 days before (22). The peritoneal cells were seeded into 6- or 12-well plates (Iwaki Glass) at a cell density of 10^6 cells/ml in 2 ml (for 6-well plates) or 1 ml (for 12-well plates) of RPMI medium (Nissui) supplemented with 10% (v/v) fetal calf serum. After incubation for 2 h in a CO_2 incubator, the supernatants and nonadherent cells were removed. More than 90% of adherent cells were macrophages. Then the cells were incubated with or without 10 μg/ml LPS in medium containing 2% serum for appropriate periods. The supernatants were taken for enzyme immunoassay for prostanoids, and the cells were subjected to Western blotting (see below).

Experiments with mPGES-1 Small Interfering RNA (siRNA)—Two synthetic hairpin-forming oligonucleotides directed at mPGES-1, 5′-GATCCCGGCCTTTGCCAACCCCGAGTTCAAGAGACTCGGGGTTGGCAAAGGCCTTTTTTGGAAA-3′ (sense) and 3′-AGCTTTTCCAAAAAAGGCCTTTGCCAACCCCGAGTCTCTTGAACTCGGGGTTGGCAAAGGCCGG-5′ (antisense), both of which harbored BamHI and HindIII sites at their 5′- and 3′-ends, respectively, were annealed, cut with BamHI and XbaI, and then ligated into the BamHI/XbaI-digested pRNA-U6.1/Hygro vector (GenScript) using T4 ligase (Takara Biomedicals). After transformation into DH5α-competent cells (TOYOBO), the plasmid was extracted and purified using the Endofree Plasmid Maxi Kit (Qiagen).

Transfection of the plasmid into peritoneal macrophages was performed by lipofection, as described previously (4). Briefly, 5 μg of the plasmid was mixed with 10 μl of LipofectAMINE 2000 (Invitrogen) in 100 μl of Opti-MEM (Invitrogen) for 30 min and then added to macrophages in 0.5 ml of Opti-MEM in 12-well plates. After incubation for 24 h, the medium was replaced with 1 ml of fresh culture medium and then incubated with or without 10 μg/ml LPS in medium containing 2% fetal calf serum for 16 h.

Acetic Acid Writhing Reaction—The writhing reaction was induced in mice by intraperitoneal injection of 0.9% (v/v) acetic acid solution at a dose of 5 ml/kg, as described previously (23, 24). In one group of animals, LPS (10 μg/0.1 ml of saline/mouse) was given intraperitoneally 18 h before the injection of acetic acid solution. A suspension of 1 mg/ml indomethacin in 1% (w/v) sodium carboxymethylcellulose solution was injected subcutaneously into mice (at final dose of 10 mg/kg indomethacin/mouse) 30 min before the injection of acetic acid solution. The number of writhing responses was counted every 5 min.

For measurement of prostanoids, mice were sacrificed 15 min after acetic acid injection, and their peritoneal cavities were washed twice with Hanks' balanced salt solution (Nissui) containing 10 μM indomethacin. The pooled peritoneal fluids were adjusted to pH 3.0 with 1 N HCl and passed through Sep-Pak C18 cartridges (Waters), and the retained PGs were eluted from the cartridges with 8 ml of methanol, as described previously (23, 24). A trace amount of [^{3}H]PGE_2 (Cayman Chemicals) was added to the samples before passage through the cartridges to calibrate the recovery of PGs. The solvent of the samples was evaporated, and then PGs were dissolved in an aliquot of buffer and assayed with commercial enzyme immunoassay kits for each PG.

Cotton Thread-induced Granulation Tissue Formation—Cotton threads (Araiwa Co.) were washed overnight with ethyl acetate and dried at room temperature before being cut into 1-cm lengths (3 mg weight), and sterilized by dry heat at 180 °C for 2 h. The cotton threads were implanted subcutaneously into the dorsum of anesthetized mice by using a 13-gauge implant needle (Natume), as described previously (25). After appropriate periods, the mice were anesthetized and killed, and the granulation tissues were dissected together with the cotton threads and weighed. As required for the experiments, indomethacin (5 mg/kg) or vehicle was injected intraperitoneally every day. The isolated granulation tissues were washed, cut into small pieces with scissors, and homogenized with a Polytron homogenizer in a homogenizing buffer comprising 20 mM Tris-HCl (pH 7.4), 250 mM sucrose, 0.5 mM EDTA, 10 μM indomethacin, 1 μM phenylmethylsulfonyl fluoride, and 0.5% (v/v) Triton X-100. The obtained tissue homogenates were centrifuged at 3,000 rpm for 5 min, and 200-μl aliquots of the supernatants were centrifuged again at 14,000 × *g* for 30 min at 4 °C. Then, the hemoglobin concentrations in the supernatants were determined spectrophotometrically by measuring the absorbance at 540 nm with a hemoglobin assay kit (Wako). PGs were extracted from the homogenates with Sep-Pak C18 cartridges and quantified by enzyme immunoassay, as described above.

Western Blotting—Aliquots of samples (20-μg protein equivalents) were subjected to SDS-PAGE using 7.5% (for $cPLA_2\alpha$ and COXs) or 12.5% (for PGESs) gels under reducing conditions. The separated proteins were electroblotted onto nitrocellulose membranes (Schleicher & Schuell) with a semidry blotter (MilliBlot-SDE system; Millipore). After blocking with 3% (w/v) skim milk in Tris-buffered saline (TBS (pH 7.4)) containing 0.05% Tween 20 (TBS-Tween), the membranes were probed with the respective antibodies (1:5,000 dilution for $cPLA_2\alpha$, COX-2, and PGESs; 1:1,000 dilution for VEGF; 1:2,500 dilution for HDC, and 1:20,000 dilution for COX-1 in TBS-Tween) for 2 h, followed by incubation with horseradish peroxidase-conjugated anti-mouse (for $cPLA_2\alpha$), anti-rabbit (for PGESs and HDC), or anti-goat (for COXs and VEGF) IgG antibody (1:5,000 dilution in TBS-Tween) for 2 h, and were visualized with the ECL Western blot system (PerkinElmer Life Sciences), as described previously (4).

Immunohistochemistry—Formalin-fixed, paraffin- embedded sections of the granulation tissue sections were incubated with Target Retrieval Solution (DAKO) as required, incubated for 10 min with 3% (v/v) H_2O_2, washed three times with TBS for 5 min each, incubated for 30 min with 5% (v/v) skim milk, washed three times with TBS-Tween for 5 min each, and incubated for 2 h with anti-mPGES-1 antibody in TBS (1:100 dilution). After five washes, the sections were treated with the CSA system staining kit (DAKO) followed by counterstaining with hematoxylin and eosin, as described previously (12).

Arthritis Model—Arthritis was induced in mPGES-1 KO and WT mice by the modified method of Terato *et al.* (26, 27). Briefly, mice were injected intraperitoneally with 10 mg of anti-type II collagen monoclonal antibodies (Immuno-Biological Laboratory) on day 0. On days 2 and 7, 50 μg of LPS (100 μl of 500 μg/ml solution in saline) was injected intraperitoneally followed by an intermittent LPS injection every 3 days to the end of the experiments. As a control, 2.5 or 0.1 ml of saline was injected in place of the antibodies or LPS, respectively. The clinical

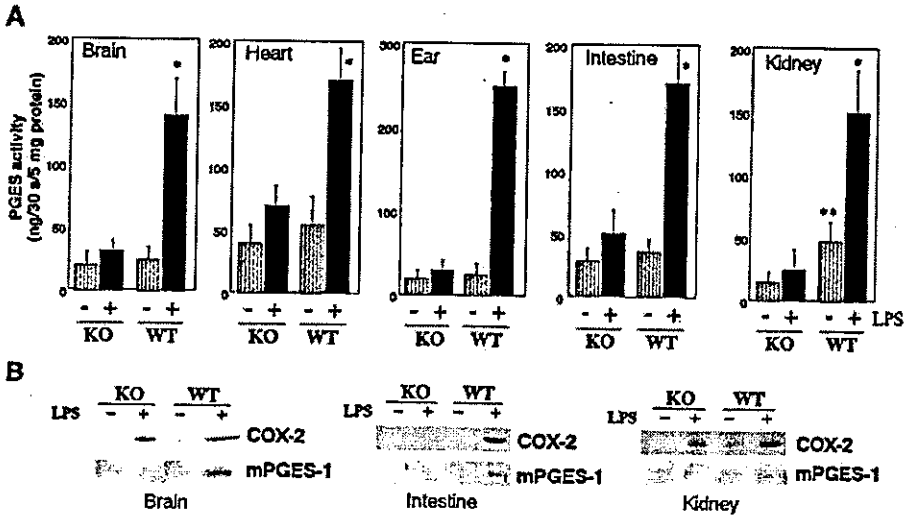

FIG. 1. **PGES enzymatic activities in tissues of WT and mPGES-1 KO mice.** *A*, tissues from WT and mPGES-1 KO mice treated for 24 h with (+) or without (−) LPS were homogenized, and PGES enzymatic activities in their membrane fractions were assessed. *, $p < 0.05$ *versus* each LPS-untreated group of WT mice; **, $p < 0.05$ *versus* LPS-untreated kidney of KO mice ($n = 3$–4). *B*, expression of mPGES-1 in several tissues of WT and KO mice with or without LPS treatment as assessed by Western blotting. Representative results of three or four independent experiments are shown.

severity of arthritis was graded on a 0–3 scale as follows: 0, normal; 1, swelling of ankle or wrist, or limited to digits; 2, swelling of the entire paw; 3, maximal swelling. Each limb was graded by a single blinded observer, allowing a maximum arthritis score of 12 for each animal. On day 28, the mice were anesthetized with ketamine/xylazine solution and a radiograph was taken with a soft x-ray apparatus (CMB-2; SOFTEX). After perfusion of mice with 4% (w/v) buffered paraformaldehyde, fore and right hind limbs were removed, decalcified in 10% (w/v) EDTA, and embedded in paraffin, and 5-μm sections were stained with hematoxylin and eosin or toluidine blue. Bone resorption was evaluated by the tartrate-resistant acid phosphatase (TRAP) staining of the carpometacarpal joints. TRAP-positive cells were stained at pH 5.0 in the presence of L(+)-tartaric acid using naphthol AS-MX phosphate (Sigma) in *N,N*-dimethylformamide as the substrate. The specimens were subjected to histomorphometric analyses using a semiautomated system (Osteoplan II; Carl Zeiss), and measurements were made at a magnification of ×400. Osteoclast number and eroded surface were measured at the carpometacarpal joints in the metacarpal bones.

After perfusion fixation, left femora and tibiae were excised and bone mineral density (BMD) was measured by dual energy x-ray absorptiometry using a bone mineral analyzer (DCS-600; Aloka Co.). To evaluate bone destruction of the knee joint area, BMDs of four equal longitudinal divisions in femur and tibia were measured, and the BMD around the knee joint was expressed by the sum of those in the distal one-fourth of femur and in the proximal one-fourth of tibia (28).

On day 6, all four paws including wrist or ankle joints were collected and homogenized in a homogenizing buffer. Then, aliquots were taken for PGE_2 enzyme immunoassay and Western blotting, as described above.

Other Methods—Protein concentrations were determined by a bicinchoninic acid protein assay kit (Pierce) with bovine serum albumin (Sigma) as a standard. Data were analyzed by Student's *t* test. Results are expressed as the mean ± S.E., with $p = 0.05$ as the limit of significance.

RESULTS

mPGES-1 Is a Major Inducible PGES in Vivo—Fig. 1*A* illustrates PGES enzymatic activities in the membrane fraction of various tissues from mPGES-1 KO and WT mice with or without 24-h treatment with LPS. Basal PGES activities (*i.e.* without LPS administration) in the brain, heart, intestine, and ear were similar between WT and KO mice, whereas the activity in the kidney of WT mice was about 4-fold higher than that of KO mice (Fig. 1*A*). Treatment of WT mice with LPS resulted in 3–8-fold increases in PGES activity over the basal levels of the individual tissues. In tissues of mPGES-1 KO mice, LPS-stimulated increases in PGES activity over the basal levels were only modest, although <2-fold increases were consistently observed in all tissues examined (Fig. 1*A*).

Immunoblotting of the membrane fractions of individual tissues revealed that the expression of mPGES-1 was markedly induced in tissues of WT mice, whereas no mPGES-1 protein was detected in tissues of KO mice (Fig. 1*B*). Constitutive expression of mPGES-1 was seen only in the kidney of WT mice (Fig. 1*B*), in agreement with a recent immunohistochemical study demonstrating the expression of mPGES-1 in the epithelia of distal tubules and medullary collecting ducts in this organ (29). In the brain (Fig. 1*B*), heart, and ear (data not shown), LPS-induced COX-2 expression in KO mice was similar to that in WT mice. In the intestine and kidney, COX-2 expression in LPS-treated KO mice was significantly lower than that in replicate WT mice (Fig. 1*B*), suggesting that mPGES-1-derived PGE_2 amplifies COX-2 induction in these tissues. Thus, mPGES-1 represents a major inducible membrane-associated PGES in various tissues of LPS-treated mice. However, the fact that substantial levels of PGES activity still exist in tissues of KO mice implies the presence of another membrane-bound PGES that is expressed rather constitutively.

Evaluation of the Role of mPGES-1 in PGE_2 Production by LPS-stimulated Macrophages—Accumulating evidence suggests that delayed PGE_2 production by LPS-stimulated macrophages depends on inducible COX-2 and mPGES-1 (4, 20, 22). To reevaluate the contribution of mPGES-1 to this event, we first took advantage of siRNA technology. As shown in Fig. 2*A*, *ex vivo* stimulation of C57BL/6 mouse-derived thioglycollate-induced peritoneal macrophages with LPS led to a marked increase in PGE_2 production, which was accompanied by *de novo* induction of COX-2 and mPGES-1. This PGE_2-biosynthetic response was reduced dramatically in replicate cells transfected with mPGES-1 siRNA, in which mPGES-1 expression was greatly decreased without reduction of COX-2 expression (Fig. 2*A*). This indicates that mPGES-1 contributes to the production of the majority of PGE_2 in LPS-stimulated macrophages.

Consistent with this observation, LPS-stimulated PGE_2 production was impaired markedly in macrophages derived from mPGES-1 KO mice relative to those derived from WT mice over the entire culture period (Fig. 2*B*). Constitutive expression of

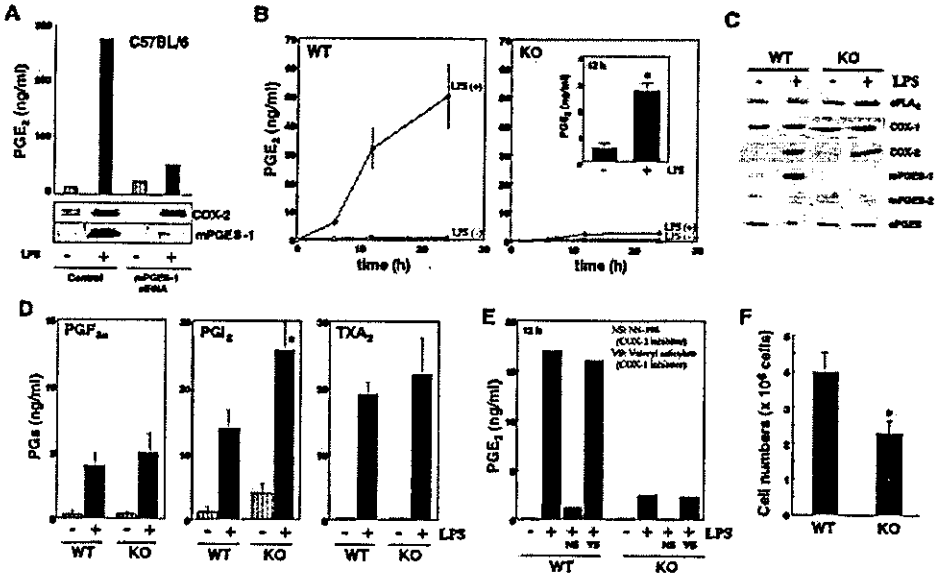

FIG. 2. **mPGES-1 is an essential component for PGE_2 production by LPS-stimulated macrophages.** *A*, peritoneal macrophages derived from C57BL/6 mice were transfected with mPGES-1 siRNA or mock control and then treated for 24 h with (+) or without (−) LPS. PGE_2 released into the supernatants was quantified. Cells were subjected to Western blotting for COX-2 and mPGES-1 (*bottom*). *B*, peritoneal macrophages obtained from WT and mPGES-1 KO mice were incubated for the indicated periods with or without LPS to assess PGE_2 release. PGE_2 production by KO macrophages is magnified in the *inset*. *C*, Western blotting of the PGE_2 biosynthetic enzymes in WT- and KO-derived macrophages after 24-h culture with (+) or without (−) LPS. *D*, production of other PGs by WT and KO macrophages after 24-h culture with (+) or without (−) LPS. *E*, effects of COX isozyme-selective inhibitors on LPS-stimulated PGE_2 production by WT and KO macrophages. *F*, numbers of macrophages recovered from the peritoneal cavities of thioglycollate-treated WT and KO mice. In *B*, *D*, and *F*, values are the mean ± S.E. of four independent experiments. A representative result of two reproducible experiments is shown in *A*, *C*, and *E*.

$cPLA_2\alpha$, COX-1, cPGES, and mPGES-2 (appearing as a doublet, reflecting the processed and unprocessed forms (16)) and inducible expression of COX-2 were similar between WT- and KO-derived macrophages (Fig. 2*C*), indicating that mPGES-1 deficiency does not affect the expression of other enzymes implicated in PGE_2 synthesis in these cells. The levels of other prostanoids, including $PGF_{2\alpha}$, thromboxane A_2, and particularly PGI_2, produced by mPGES-1 KO cells were modestly higher than those produced by WT cells (Fig. 2*D*), which may reflect a shunting effect because of the defect of the metabolic flow from PGH_2 to PGE_2.

It should be noted, however, that a small but significant production of PGE_2 was still observed in mPGES-1-deficient macrophages (Fig. 2*B*). The level of PGE_2 released by mPGES-1-null macrophages reached as much as 8% of that produced by WT cells after 12-h culture with LPS (Fig. 2*B*, *inset*). To assess which COX isoforms contribute to PGE_2 production in mPGES-1-deficient macrophages, the effects of specific inhibitors of COX-1 (valeryl salicylate) and COX-2 (NS-398) on PGE_2 generation were examined. As shown in Fig. 2*E*, PGE_2 production was reduced markedly by NS-398, whereas valeryl salicylate was without effect in both WT and KO cells. This result indicates that the small production of PGE_2 observed in mPGES-1-null macrophages still depends largely on COX-2. Because mPGES-2 and cPGES were expressed in these cells (Fig. 2*C*), this small PGE_2 production might occur through these enzymes.

During the course of this study, we noted that the number of macrophages recovered from the peritoneal cavity 4 days after the injection of thioglycollate was significantly lower in mPGES-1 KO mice than in WT mice (Fig. 2*F*). This result suggests that mPGES-1-derived PGE_2 may participate in the migration of macrophages into inflamed sites, an event also found in the model of inflammatory granulation tissue formation (see below).

Participation of mPGES-1 in Pain Nociception—During the inflammatory reaction, pain is produced through complex interactions between various inflammatory mediators, one of which is PGE_2. Studies using COX inhibitors as well as PG receptor-deficient mice have established the important role of PGE_2 as well as PGI_2 in pain nociception (24, 30–32). We therefore used the acetic acid writhing test to evaluate the contribution of mPGES-1 to the production of PGE_2 involved in nociceptive pain perception. We were particularly interested in inflammatory pain hypersensitivity in LPS-pretreated animals because the expression levels of both COX-2 and mPGES-1 are markedly elevated after LPS treatment (Figs. 1 and 2).

Injection of acetic acid into the peritoneum of WT mice induced stretching behavior, which peaked at 5–10 min and then declined gradually over 30 min (Fig. 3*A*, *upper panel*). This basal writhing response was augmented significantly at all time points if LPS had been injected into mice 24 h before acetic acid injection (Fig. 3*A*, *lower panel*). Notably, the LPS-primed, acetate-induced pain response was reduced markedly in mPGES-1 KO mice compared with that in replicate WT mice over the entire experimental period (Fig. 3*B*, *lower panel*). Under LPS-unprimed (basal) conditions, the writhing response of mPGES-1 KO mice was also significantly less than that of WT mice (Fig. 3*B*, *upper panel*), although the difference between WT and KO mice was less obvious than that observed after LPS priming. Thus, the total numbers of stretching of mPGES-1 KO mice over the initial 15 min after acetic acid administration were reduced by ~45 and ~80% relative to those of WT mice under basal and LPS-primed conditions, respectively (Table I). Both the basal and LPS-primed writhing responses of WT mice were reduced by 70–80% by treatment with indomethacin (Fig. 3*C*). These results collectively suggest that mPGES-1-derived PGE_2 is a main mediator of LPS-primed pain hypersensitivity, whereas the basal pain response may also involve PGE_2 produced by other PGES(s) or other additional prostanoid(s) such as PGI_2, because this pain response is reduced markedly in mice lacking the PGI receptor IP (24, 30).

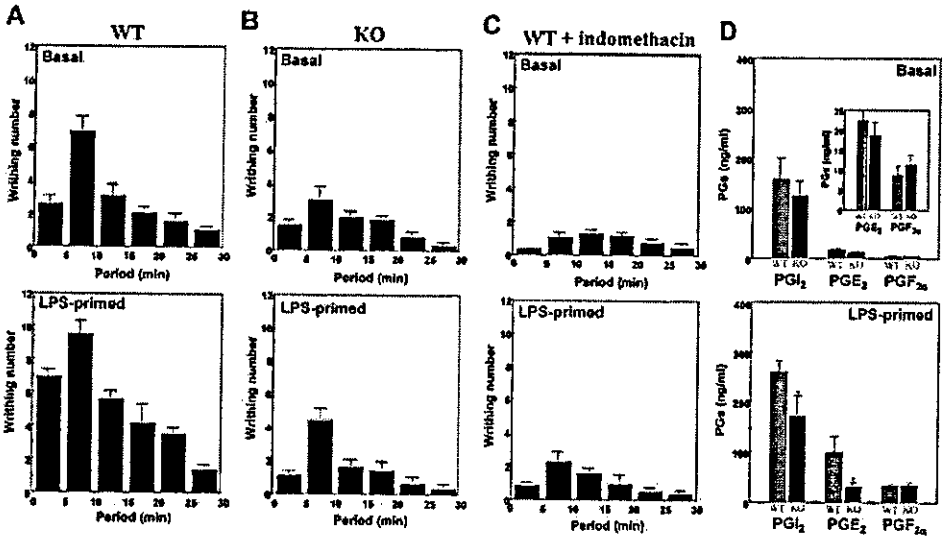

FIG. 3. **Impaired pain hypersensitivity in mPGES-1-deficient mice.** *A–C*, the acetic acid writhing reaction of WT (*A* and *C*) and mPGES-1 KO (*B*) mice before (*upper*) and 24 h after (*lower*) treatment with LPS. In *C*, indomethacin was administered to WT mice 2 h before acetic acid challenge. Values are the mean ± S.E. (n = 12–13; *, $p < 0.05$). *D*, levels of prostanoids in the peritoneal cavities of LPS-primed (*lower*) and unprimed (*upper*) mice 15 min after injection of acetic acid. Levels of PGE_2 and $PGF_{2\alpha}$ in LPS-unprimed mice are magnified in the *inset*. Values are the mean ± S.E. (n = 7; *, $p < 0.05$).

TABLE I
Reduced pain response in mPGES-1 KO mice

The total numbers of writhing reaction over the initial 15 min after the acetic acid administration are shown. Values are the mean ± S.E. (n = 12–13). *, $p < 0.05$ *versus* WT without LPS priming; **, $p < 0.05$ *versus* respective WT control. IM, indomethacin.

Mice	LPS priming	Writhing numbers
WT	−	10.3 ± 0.9
WT	+	20.1 ± 2.4 *
KO	−	5.5 ± 0.6**
KO	+	7.1 ± 0.6**
WT + IM	−	3.0 ± 0.8**
WT + IM	+	4.5 ± 0.6**

In WT mice, the level of PGE_2 in the peritoneal cavity 15 min after acetic acid injection was about 6-fold higher in the LPS-primed group than in the LPS-unprimed group (Fig. 3*D*), in agreement with the elevated expression of COX-2 and mPGES-1 in response to LPS (see Figs. 1 and 2). In mPGES-1 KO mice, peritoneal PGE_2 levels were reduced only by ~15% (this difference was statistically insignificant) and by as much as ~70% compared with those in WT mice under the basal and LPS-primed conditions, respectively (Fig. 3*D*). Given that the reduction of the peritoneal PGE_2 level is less marked than that of the writhing response in KO mice, particularly under LPS-unprimed condition, we speculate that PGE_2 produced in the spinal cord and dorsal root ganglia, in which a trace level of mPGES-1 is constitutively expressed (33), might also affect pain perception by spinal neurons. As reported previously (23, 24), PGI_2 is the major prostanoid released into the peritoneal cavities of mice during the acetic acid writhing response with or without LPS priming (Fig. 3*D*). Consistent with the elevation of COX-2 expression after LPS treatment, the peritoneal PGI_2 level was 1.8-fold higher in LPS-treated than in untreated WT mice (Fig. 3*D*). Interestingly, the levels of PGI_2 in mPGES-1 KO mice were significantly lower than in WT mice after LPS priming (Fig. 3*D*), suggesting partial dependence of PGI_2 synthesis on mPGES-1-derived PGE_2 in this setting. Production of $PGF_{2\alpha}$ was increased 3-fold after LPS priming and was unaffected by mPGES-1 deficiency in both basal and LPS-primed situations (Fig. 3*D*). The greater -fold increase in $PGF_{2\alpha}$ than in PGI_2 after LPS treatment may reflect distinct functional coupling between COX-2 and various terminal synthases (34) or LPS-mediated induction of $PGF_{2\alpha}$ synthase (35). Indomethacin treatment of WT mice reduced the peritoneal PGI_2 levels by >90% with or without LPS priming (data not shown), indicating that the reduced writhing response by indomethacin (Fig. 3*C*) is related to almost complete inhibition of COX enzymes.

Participation of mPGES-1 in Inflammatory Granulation and Angiogenesis—Subcutaneous implantation of a cotton thread in the dorsum of mice induces formation of granulation tissue with angiogenesis (25). As shown in Fig. 4*A*, granulation tissue formation and angiogenesis around the implanted cotton thread were obvious in C57BL/6 mice, events that were ameliorated in replicate mice treated with indomethacin, implying the involvement of prostanoid(s). Quantification studies revealed that the weights of and the levels of hemoglobin (an indicator of angiogenesis) and PGE_2 in the granulation tissue were reduced significantly in indomethacin-treated mice compared with vehicle-treated mice (Fig. 4*B*).

To evaluate the contribution of mPGES-1 to this inflammatory process, cotton threads were implanted into the dorsum tissues of mPGES-1 WT and KO mice. As in the case of C57BL/6 mice, progressive formation of granulation tissue and vascular networks in the subcutaneous tissues around the implanted cotton thread was visually obvious in WT mice, and this process peaked on day 5 (Fig. 4*C*). In comparison, formation of granulation tissue and blood vessels appeared mild in mPGES-1-deficient mice (Fig. 4*C*). Accordingly, there was a significant increase in the wet weight of the cotton thread-associated granulation tissue in WT mice over days 5–7, whereas this increase was not observed appreciably in mPGES-1 KO mice (Fig. 4*D*, *left panel*). Angiogenesis, as quantified by hemoglobin levels, in the granulation tissue peaked on days 3–5 in WT mice and then declined, and there was ~50% reduction in hemoglobin levels in KO mice relative to WT mice (Fig. 4*D*, *middle panel*). PGE_2 levels in the granulation tissue of WT mice peaked on days 1–3 and then declined (Fig. 4*D*, *right panel*). Thus, it appears that increased PGE_2 production kinetically precedes angiogenesis, followed by granulation tissue formation in WT mice. In mPGES-1 KO mice, PGE_2 levels were almost constant throughout the experimental period, and

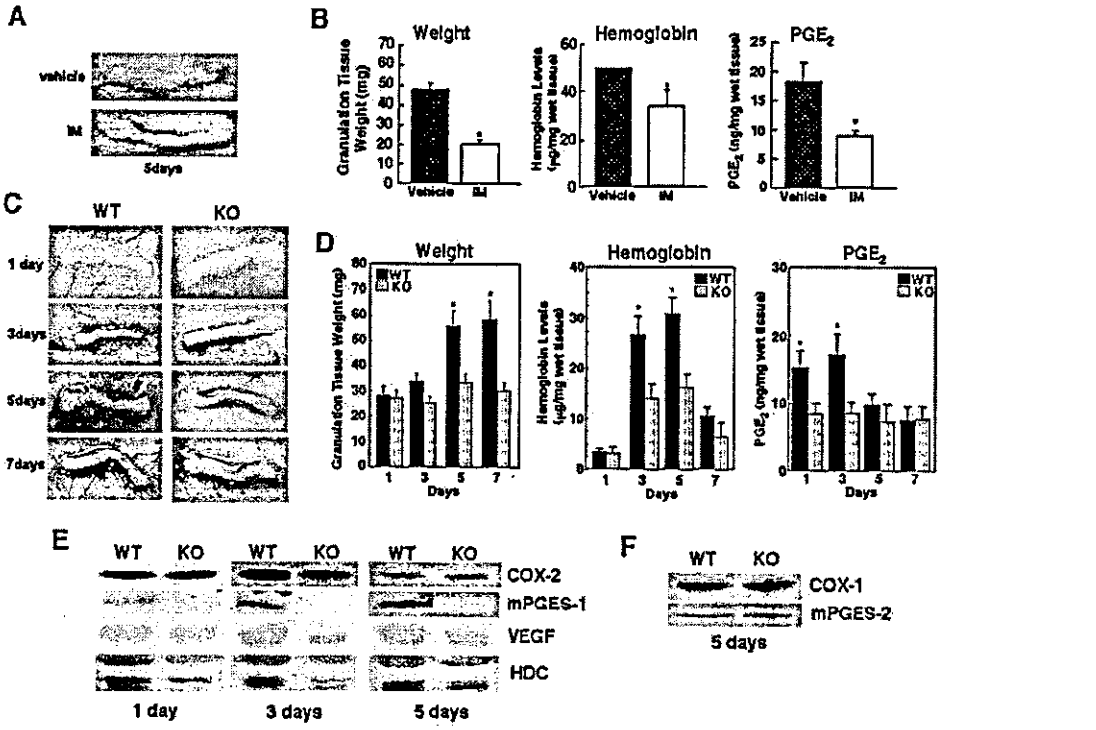

FIG. 4. **Reduced inflammatory granulation tissue formation and angiogenesis in mPGES-1 KO mice.** *A* and *B*, a cotton thread was implanted subcutaneously in the dorsum of C57BL/6 mice with or without indomethacin (*IM*) treatment. After taking photographs on day 5 (*A*), changes in wet weights of, and hemoglobin and PGE_2 levels in, the isolated granulation tissues were quantified (*B*). Values are the mean ± S.E. ($n = 7$; *, $p < 0.05$ *versus* replicate WT mice). *C–F*, a cotton thread was implanted subcutaneously in the dorsum of WT and mPGES-1 KO mice. Photographs indicate granulation tissues and vascular networks around the cotton thread on days 1, 3, 5, and 7 (*C*), and changes in wet weights of, and hemoglobin and PGE_2 levels in, the granulation tissues were quantified (*D*). Values are the mean ± S.E. ($n = 12–13$; *, $p < 0.05$ *versus* replicate KO mice). The time course of expression of COX-2, mPGES-1, VEGF, and HDC by day 5 (*E*) and the expression of COX-1 and mPGES-2 on day 5 (*F*) in the granulation tissues were assessed by immunoblotting. Representative results of more than five experiments are shown in *A*, *C*, *E*, and *F*.

there was no increase in PGE_2 during days 1–3 (Fig. 4*D*, *right panel*). On day 7, the hemoglobin and PGE_2 levels in the granulation tissue of WT mice returned to levels comparable with those of KO mice (Fig. 4*D*).

As assessed by immunoblotting, COX-2 and mPGES-1 were not expressed in the normal dorsum of WT mice (data not shown) and were markedly induced in the granulation tissue formed after cotton thread implantation (Fig. 4*E*). The inducible expression of COX-2 reached a peak on days 1–3 and then declined (Fig. 4*E*), thus roughly coinciding with the levels of PGE_2 in the granulation tissue (Fig. 4*D*, *right panel*). The expression level of COX-2 was slightly higher in WT mice than in KO mice on day 3. The expression of mPGES-1 reached a plateau peak on days 3–5 in WT mice, whereas mPGES-1 was absent from KO mice over the whole period (Fig. 4*E*). Expression of COX-1 and mPGES-2 was unchanged over the experimental period and was similar between WT and KO mice (Fig. 4*F*).

Granulation tissue formation and angiogenesis observed in this model depend on the up-regulation of VEGF, an essential angiogenic factor, and HDC, an enzyme required for the synthesis of histamine (25). We therefore assessed by immunoblotting the expression of VEGF and HDC in the granulation tissue of mPGES-1 KO and WT mice. Although the expression levels of VEGF were similar between WT and KO mice on day 1, there were significant elevations in VEGF expression in WT mice compared with KO mice on days 3–5 (Fig. 4*E*). The expression levels of HDC, which appeared as 70- and 55-kDa forms, were significantly higher in WT mice than in KO mice over the whole experimental periods (Fig. 4*E*). These results suggest that mPGES-1-derived PGE_2 plays an augmentative role in the expression of VEGF and HDC.

Histological analyses of the granulation tissues revealed the presence of a fibroblastic layer around the implanted cotton thread, which was thicker in WT mice than in mPGES-1 KO mice (Fig. 5, *A* and *B*). The smooth muscle layer in WT mice was edematous, an event that was less clear in KO mice (Fig. 5*A*). In addition, more capillary vessels were found in the fibroblastic layer of WT mice than in that of KO mice (Fig. 5*B*). For quantification of capillary vessel formation, we took seven digital images of randomly selected areas of the granulation tissue of WT and KO mice, and the numbers of capillary vessels and the pixels of vessel areas (as an indication of vessel volumes) were evaluated. As a result, the numbers of capillary vessels of WT and KO mice/digital image were 23.3 ± 4.7 and 11.7 ± 1.4 ($p < 0.05$), respectively, and the pixel numbers were 9,800 ± 1,500 and 4,200 ± 750 ($p < 0.05$), respectively, thus revealing ~50% reduction in capillary vessel formation (in terms of both numbers and sizes) in KO mice compared with WT mice. Immunohistochemical staining of these tissues with anti-mPGES-1 antibody showed that mPGES-1 immunoreactivity was distributed mainly in macrophages infiltrating into the fibroblast layer of WT mice (Fig. 5, *C* and *D*). Fewer macrophages were found in replicate KO mice, from which mPGES-1 immunoreactivity was absent.

Participation of mPGES-1 in Inflammatory Arthritis—Experimental and clinical evidence suggests that PGE_2 is a critical mediator of rheumatoid arthritis in humans and in related animal models (36–42). Therefore, we next examined the contribution of mPGES-1 to collagen antibody-induced arthritis

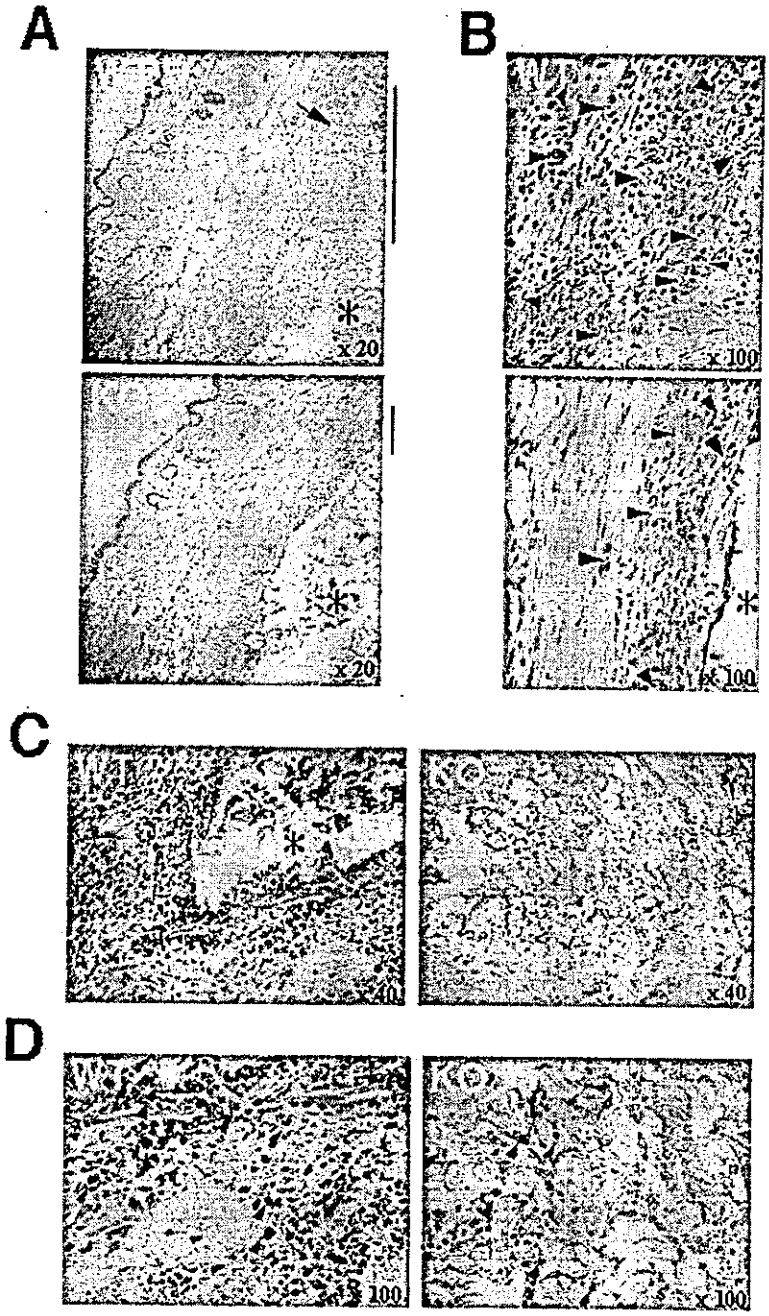

FIG. 5. **Histological analyses of cotton thread-induced granulation tissues.** *A* and *B*, hematoxylin and eosin staining of the 5-day granulation tissues from WT and KO mice at low (*A*) and high (*B*) magnifications. *Arrow* and *asterisks* in *A* indicate the edematous lesion in the smooth muscle layers and the positions of the implanted cotton thread, respectively. *Arrowheads* in *B* indicate capillary vessels in the fibroblastic layers. *C* and *D*, immunohistochemical staining of the granulation tissues with anti-mPGES-1 antibody at low (*C*) and high (*D*) magnifications. Scattered staining of mPGES-1 was found in WT, but not KO, mice. *Asterisk* in *C* indicates the position of the cotton thread, and *arrowheads* in *D* indicate macrophage-like cells.

(CAIA), an experimental animal model for human rheumatoid arthritis. Compared with classical collagen-induced arthritis (CIA), the induction of which is limited to only a few strains such as DBA/1 (43), the CAIA model has the great advantages of applicability to various strains, rapid induction, and high incidence of arthritis. To this end, a mixture of anti-type II collagen monoclonal antibodies was administered to mPGES-1 KO and WT mice with C57BL/6 × 129/SvJ background. However, after application of the antibody mixture plus only one injection of LPS (on day 2), active inflammation declined after 2 weeks so that we were unable to observe obvious bone destruction radiographically (data not shown). We therefore performed booster injections of LPS into these mice every 3 days from day 7, which eventually allowed sustained arthritic inflammation over 4 weeks.

The arthritis score in WT mice began to rise on day 4, reaching a peak value (score ~7) on days 7–10, and then decreased gradually to a still elevated score of >5 by 4 weeks (Fig. 6*A*). Although replicate mPGES-1 KO mice also developed arthritic symptoms during the same period, there was a significant reduction in the severity of the disease in mPGES-1 KO mice compared with WT mice (40~50% reduction from days 7 to 28). In contrast to the reduced severity, however, the incidence of arthritis was 100% in both WT and KO mice. On day 6, when the arthritis was developing (Fig. 6*A*), PGE_2 levels in all four paws of arthritis-induced WT and KO mice were increased significantly over those in their respective saline control groups (Fig. 6*B*). Importantly, there was a ~50% reduction in the PGE_2 level in arthritis-induced KO mice relative to that in replicate WT mice (Fig. 6*B*). As assessed by immunoblotting,

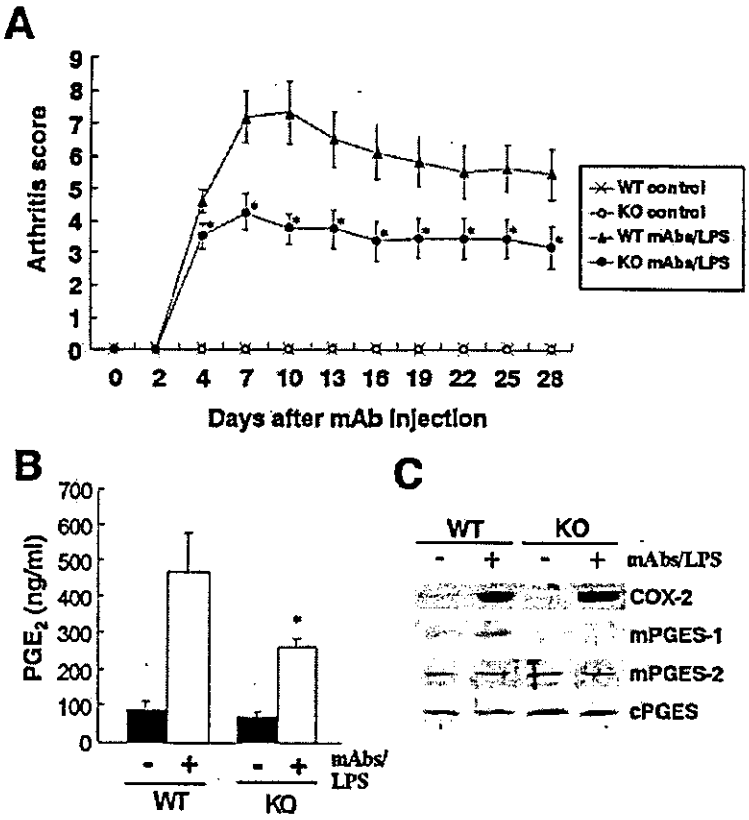

FIG. 6. **Reduced severity of CAIA in mPGES-1 KO mice.** mPGES-1 KO and WT mice were injected with anti-collagen monoclonal antibodies (*mAb*) on day 0 and boosted with LPS on days 2 and 7, followed by intermittent LPS injections every 3 days. *A*, the clinical arthritis score was graded on a 0–3 scale as described under "Experimental Procedures." Values are the mean ± S.E. (n = 10–11; *, $p < 0.05$ *versus* monoclonal antibody/LPS-treated WT mice on each day). *B* and *C*, all four paws of mice in each group were removed on day 6, and homogenized tissues were subjected to PGE_2 measurement (*B*) and Western blotting (*C*). In *B*, values are the mean ± S.E. (n = 3; *, $p < 0.05$ *versus* replicate WT mice).

the expression of COX-2 and mPGES-1 was increased markedly, whereas that of mPGES-2 and cPGES remained unchanged, in arthritis-induced WT mice (Fig. 6*C*). In mPGES-1 KO mice, the inducible expression of COX-2 and constitutive expression of cPGES and mPGES-2 were similar to those in WT mice, whereas mPGES-1 was absent.

Histopathological examination using knee joint sections of arthritis-induced mice on day 28 revealed notable joint destruction in WT mice (Fig. 7*A*, *upper two panels*). Cartilage degeneration was also evident in the toluidine blue-stained sections (Fig. 7*A*, *lower two panels*), which is suggestive of significant proteoglycan loss in articular cartilage of WT mice. In contrast, these histopathological changes were rather mild in arthritis-induced KO mice (Fig. 7*A*, *right panels*). We further compared the arthritis-induced bone loss between the two genotypes by measuring BMD of the periarticular region. The decrease in BMD of diseased WT mice relative to control WT mice was nearly 20%, whereas that of KO mice was only 12%, thereby revealing about 40% less BMD loss in KO mice than in WT mice (Fig. 7*B*).

Fig. 7*C* shows radiographs of forepaws and histologies of the TRAP staining of the metacarpal bones in arthritis-induced WT and KO mice on day 28. Bone erosion and periositis were obvious in WT mice but were not clear in KO mice. Furthermore, histomorphometric parameters of bone resorption, namely osteoclast number and percent eroded surface, were much more increased by arthritis in WT mice than in KO mice (Fig. 7*D*). Collectively, these results indicate that mPGES-1-derived PGE_2 may be involved in development of CAIA and the accompanying joint destruction.

DISCUSSION

In keeping with various pathophysiological roles of PGE_2, as demonstrated by pharmacological inhibition and gene targeting of COX-2 and the four PGE receptors EP1–EP4 (1, 2), we used mPGES-1-deficient mice (20) to evaluate the *in vivo* functions of mPGES-1, a terminal PGE_2-biosynthetic enzyme that is markedly up-regulated during inflammatory responses (3–14). We provide unequivocal evidence that mPGES-1 plays a pivotal role in the production of PGE_2 linked to inflammatory pain hypersensitivity, inflammatory granulation associated with angiogenesis, and inflammatory arthritis accompanying bone destruction. Even though significant PGES enzymatic activity, which may be ascribed to mPGES-2, cPGES, or possibly other as yet unidentified enzymes, still exists in various tissues and cells of mPGES-1 KO mice, mPGES-1 accounts for the majority of the inducible PGES activity (Fig. 1), and importantly, it contributes far more critically to the propagation of inflammatory responses. This conclusion is supported by the facts that mPGES-1 exhibits the highest catalytic activity among the PGES enzymes identified so far (11) and that this enzyme shows preferential, if not strict, coupling selectivity with COX-2, an inducible COX isoform that has been implicated in various inflammatory disorders (4). Our results are in many aspects consistent with a recent report by Audoly and co-workers (44), who also demonstrated reduced pain nociception and inflammatory arthritis in their mPGES-1 KO mice, although there are some subtle differences in the evaluations of the results.

No doubt, PGE_2 is a critical modifier of pain nociception (24, 30, 31). It has been reported that in mice with a mixed genetic background of C57BL/6 × 129/SvJ, the PGI receptor IP mainly mediates immediate pain (30), whereas the PGE receptor EP3, in cooperation with IP, participates in pain hyperalgesia after priming with LPS (24), in the acetic acid-induced writhing model. On the other hand, another study using EP1-deficient mice of the DBA/1 background has demonstrated the striking

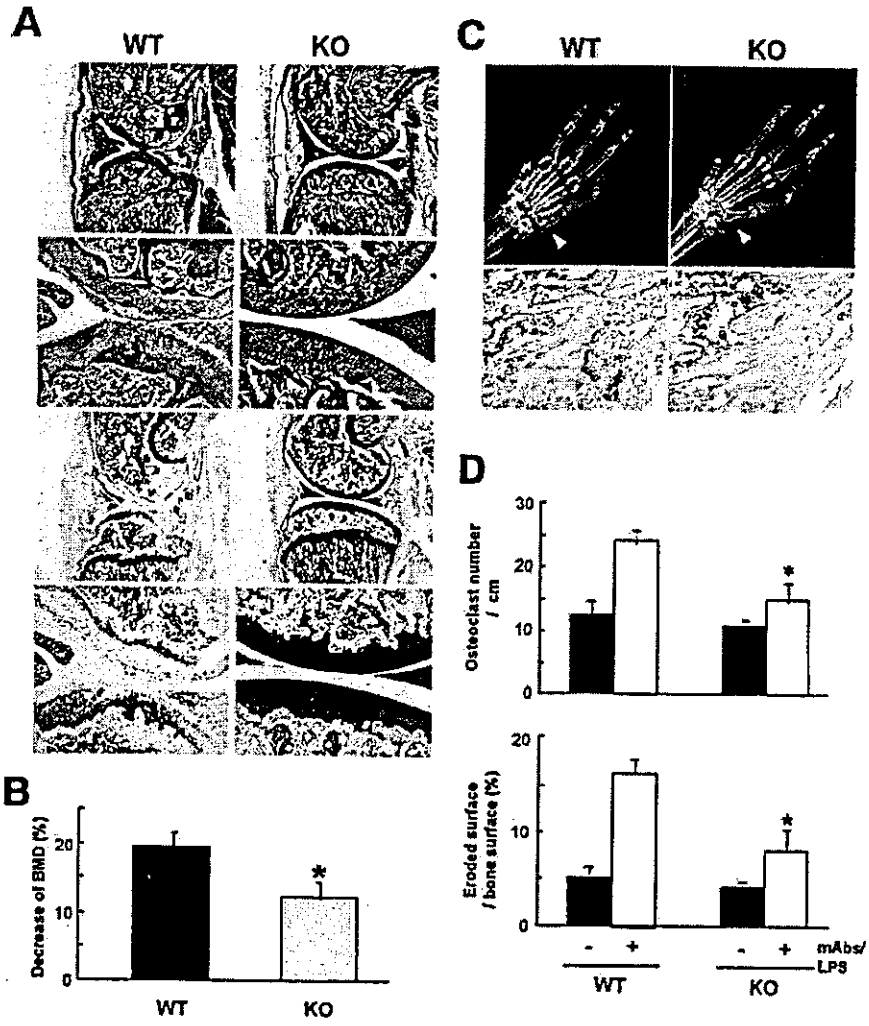

FIG. 7. **Radiological and histological findings of WT and mPGES-1 KO joints by CAIA induction.** *A*, histopathological examination of knee joint sections of arthritis-induced WT (*left panels*) and KO (*right panels*) mice on day 28, stained with hematoxylin and eosin (*upper two panels*) and toluidine blue (*lower two panels*) at low (*upper panels*; magnification, ×25) and high (*lower panels*; magnification ×100). *B*, decrease in BMD of the knee periarticular region of arthritic mice compared with control mice. BMD was measured by dual energy x-ray absorptiometry using a bone mineral analyzer. *C*, radiographs of forepaws (*upper panels*) and TRAP staining of the metacarpal bones (*lower panels;* magnification, ×200) in arthritis-induced WT and KO mice on day 28. *Arrowheads* indicate the regions where the TRAP staining and histomorphometric analysis were performed. *D*, osteoclast number (*upper panel*) and percent eroded surface (*lower panel*), which are histomorphometric parameters of bone resorption, in WT and KO mice. These parameters were measured at the carpometacarpal joints in the metacarpal bones. In *B* and *D*, values are the mean ± S.E. (n = 8–11; *, $p < 0.05$ *versus* WT mice).

contribution of this PGE receptor subtype to acute pain nociception in the same model (31). By means of the acetic acid stretching test with or without LPS priming, we have shown that mPGES-1 contributes more profoundly to LPS-primed inflammatory hyperalgesia than to basal acute pain perception (Fig. 3). Thus, ~80% suppression of the pain response and of peritoneal PGE_2 levels was observed in LPS-pretreated mPGES-1-null mice compared with replicate WT mice, which is consistent with elevated expression of COX-2 and mPGES-1 in response to LPS.

Previous studies employing COX isozyme-selective inhibitors or KO mice have indicated that COX-1, not COX-2, mainly mediates the basal acetic acid writhing reaction (32). Here we observed ~45% reduction of the basal writhing reaction in mPGES-1 KO mice relative to replicate WT mice (Fig. 3), implying a significant (even if less pronounced) contribution of preexisting mPGES-1 to COX-1-dependent acute pain. Indeed, COX-1/mPGES-1 coupling can occur in the immediate response if sufficient levels of arachidonic acid are supplied (4). However, the peritoneal PGE_2 level in KO mice was only slightly lower (statistically insignificant) than that in WT mice under the basal condition (Fig. 3*D*), suggesting that the PGE_2 produced by mPGES-1 in other sites, such as in the spinal cord and dorsal root ganglia (33), may also contribute to this response. Recently, Audoly and co-workers (44) have reported ~50% reduction in the basal writhing reaction in mPGES-1-null mice. In that study, however, the peritoneal PGE_2 level in mPGES-1 KO mice during the basal writhing response was only modestly lower than that in WT mice (44), as in our present study (Fig. 3*D*). This indicates that other PGES enzymes may also participate in this immediate PGE_2 production and possibly pain perception. In this context, mPGES-2 and cPGES, both of which can be coupled with COX-1 (16–18), may be responsible for this residual PGE_2 production, a possibility that needs to be addressed in the future.

We found significant reduction in levels of peritoneal PGI_2 in mPGES-1 KO mice relative to WT mice under the LPS-primed condition. This finding suggests the existence of a pain amplification loop, in which mPGES-1-derived PGE_2 augments the production of PGI_2, another pain modifier (24, 30). Alternatively, assuming that macrophages are the main source of these prostanoids in the writing model, decreased macrophage number at inflamed sites in mPGES-1-deficient mice (see below) may account for the reduced PGI_2 levels in these mice. The reduction of PGI_2 in mPGES-1 KO mice was not observed in the study by Audoly and co-workers (44). This discrepancy may be because they assessed only the basal pain response (but not LPS-primed pain hypersensitivity) or simply because distinct mouse strains (C57BL/6 × 129/SvJ *versus* DBA/1) were used for analyses.

Subcutaneous implantation of a cotton thread into the dorsum of the mouse induces formation of granulation tissue associated with angiogenesis (25). In this model, the process of inflammation depends on histamine, which is *de novo* synthe-

sized by HDC induced in infiltrating macrophages, and VEGF, a factor essential for new blood vessel formation. Granulation and angiogenesis are impaired in HDC-deficient mice, in which induction of VEGF in the granulation tissues is also markedly reduced (25). This model of inflammation also depends on prostanoids (45), a notion also supported by our present study showing an inhibitory effect of indomethacin (Fig. 4*A*). In this study, we found that mPGES-1 deficiency results in ameliorated granulation, edema, and angiogenesis (Figs. 4 and 5). The main cell type expressing mPGES-1 in the granulation tissues is ascribed to macrophages (Fig. 5), in which HDC is also markedly induced (25). Notably, mPGES-1-derived PGE_2 appears to be linked, at least in part, to the induction of HDC and VEGF because the expression levels of HDC and VEGF are significantly lower in mPGES-1 KO mice than in WT mice (Fig. 4*F*). The reduced angiogenesis and VEGF expression in this model seems to be reminiscent of the events observed in tumor tissues of mice deficient in the PGE receptors EP2 (46) and EP3 (47). Thus, our results indicate that mPGES-1-derived PGE_2, in cooperation with histamine and VEGF, plays a critical role in the development of inflammatory granulation and angiogenesis, thus eventually contributing to tissue remodeling.

Pharmacological and genetic evidence supports a functional link of $cPLA_2\alpha$, COX-2, and PGE_2 with human rheumatoid arthritis and its mouse experimental model, CIA (36–43). COX-2 and mPGES-1 are highly expressed in synovial lining cells of joint tissues from patients with rheumatoid arthritis (16, 48). Administration of COX-2-selective inhibitors markedly reduces the severity of disease (42, 43), and mice deficient in $cPLA_2\alpha$ (49), COX-2 (but not COX-1) (36) and the PGE receptor EP4 (50) display significant reductions in both clinical and histological signs of CIA. We now show, using a CAIA model, that the arthritic symptoms are apparently mild in mPGES-1 KO mice compared with replicate WT mice, even though the reduction of the arthritis scores in KO mice is partial (Fig. 6). Moreover, bone destruction and juxtaarticular bone loss in CAIA are less obvious in mPGES-1 KO mice than in replicate WT mice (Fig. 7). These observations are compatible with our recent finding that mPGES-1 is induced by and mediates the effects of bone-resorptive stimuli *in vitro* (51). Because mPGES-1 deficiency leads to only 50% reduction of PGE_2 level in the arthritic tissue (Fig. 6*B*), the residual PGE_2, which may result from coupling between COX-2 and other PGES(s) such as mPGES-2, may also contribute to this disease.

The inhibition of joint destruction by mPGES-1 deficiency may at least in part be secondary to the inhibition of inflammation of the joints because proinflammatory cytokines, such as tumor necrosis factor α, interleukin-1 and -6, and fibroblast growth factor-2, are known to stimulate the differentiation and activation of osteoclasts through the induction of RANKL (for receptor activator of NF-κB ligand) in osteoblasts/stromal cells (52–55). PGE_2, which is known to be induced by these cytokines, also facilitates RANKL expression (56–58). Furthermore, PGE_2 has a potency to stimulate osteoclast formation from precursors directly in the absence of osteoblasts/stromal cells (59, 60). Hence, reduced PGE_2 production by mPGES-1 deficiency in the CAIA may cause the decrease in bone destruction in both direct and indirect pathways.

While this study was under way, Audoly and co-workers (44) demonstrated a more profound contribution of mPGES-1 to another mouse arthritis model, the CIA model, in which mPGES-1-deficient DBA mice developed no or little arthritis. Interestingly, the incidence of CIA was reduced markedly in mPGES-1 KO mice in the study by Audoly and co-workers (44), whereas in our experimental setting all mPGES-1 KO mice still developed CAIA. This discrepancy may again result from differences in the mouse strains and the methods of arthritis induction employed. The CIA model employed by Audoly and co-workers (44) requires a competent adaptive immune response to chicken type II collagen and demonstrates development of anti-collagen antibodies with subsequent induction of arthritic response. In comparison, the passive CAIA approach used in this study bypasses the requirement for lymphocytes and other proximal adaptive immune responses. Audoly and co-workers (44) demonstrated that lower antibody titers were detected in mPGES-1 KO mice compared with WT mice, even though antibody levels did not necessarily correlate with onset and severity of arthritis in disease animals. Analysis of the anti-collagen antibody formation in COX-2-deficient mice reveals a remarkable decrease in this humoral response (36). This point is supported further by the observation that COX-2-deficient mice exhibit altered helper T cell development, a process reversed by PGE_2 (61). It is therefore possible that the results found in the CIA model (44) could be influenced in part by inadequate proximal lymphocyte-mediated responses in addition to the synovial symptoms. Thus, the use of the CAIA approach in our study allows a confined synovium-focused analysis and clearly demonstrates the specific role of synovial mPGES-1 in synovial inflammation.

Another interesting phenotype of mPGES-1 KO mice is the decrease in macrophage numbers at inflamed sites. Thus, in the KO mice, fewer macrophages are recovered from the peritoneal cavity after thioglycollate treatment (Fig. 2*F*) and are found immunohistochemically in the cotton thread-induced granulation tissue (Fig. 5*D*) than those in WT mice. Although this event might result simply from mitigated inflammation in mPGES-1 KO mice, which would influence subsequent recruitment of macrophages, an alternative explanation is that mPGES-1-derived PGE_2 may affect the differentiation and migration of macrophages in an as yet unidentified way. Because adhesion to the culture dishes and subsequent survival (at least by 48 h) of isolated macrophages during culture were similar between mPGES-1 KO and WT mice (data not shown), it is more likely that mPGES-1-derived PGE_2 could affect the recruitment of macrophages in tissue microenvironments. With regard to this, several recent studies have argued the potential contribution of COX-2 and PGE_2 to this process. COX-2 KO mice experience delayed hematologic recovery after 5-fluorouracil treatment, even though the basal hematopoiesis is normal (62). PGE_2 directly stimulates the *in vitro* proliferation of burst-forming unit of granulocyte-macrophage progenitors from $CD34^+$ cells (63) and regulates the production of macrophage colony-stimulating factor by bone marrow stromal cells (64). The anaphylatoxin C5a and the chemokine macrophage inflammatory protein-1α promote the recruitment of monocytes into the peritoneal cavity of mice and their subsequent differentiation into macrophages, and these events are mediated indirectly by PGE_2 (65). Moreover, PGE_2 stimulates the expression of CCR7, a receptor for the chemokine macrophage inflammatory protein-3β, on monocytes through the PGE receptors EP2 and EP4, a process required for proper homing of monocyte-derived dendritic cells to the lymph nodes (66). Thus, our present data may reflect an unexplored role of mPGES-1-derived PGE_2 in the differentiation and migration of macrophages, although further studies will be necessary to clarify this critical issue in a sophisticated approach.

Taken together, it can be concluded that mPGES-1 is involved in various types of inflammation, including pain hyperalgesia, granulation associated with angiogenesis, and inflammatory arthritis accompanying bone destruction. It should be noted that the writhe and arthritis tests involve LPS stimulation, and the degree to which this Toll-like receptor 4 agonist

influences the observed predominance of mPGES-1 in each situation has not been defined. Therefore, the generalization of the present finding to a variety of non-LPS influenced inflammatory responses (except the granulation response, which is assessed here) will need further elucidation. Irrespective of this argument, accumulating evidence suggests that mPGES-1 is also involved in tumorigenesis (12, 67), delayed skin hypersensitivity (44), and fever (68). These facts, together with its inducible property during inflammation and other pathogenesis (4–6), agree well with the proposal that mPGES-1 represents a target for the treatment of various inflammatory diseases that will spare important physiological systems in which other PGs are involved (44). However, implementation of this concept will still require caution, because besides its proinflammatory functions PGE_2 exerts homeostatic and antiinflammatory effects in several organs, such as the gastrointestinal tract (69, 70), lung (71), and kidney (72). It also remains to be elucidated whether other PGES enzymes exhibit redundant or specific functions in particular situations *in vivo*. The absence of gross abnormalities in ductus arteriosus closure immediately after birth, which is markedly impaired in COX-1/COX-2-double (73) and EP4 (74) KO mice, and in female reproduction, where EP2 is involved in the ovulation step (75), implies the compensatory participation of other PGESs in these physiological events.

Acknowledgments—We thank Dr. Satoshi Tanaka (Kyoto University) for providing anti-HDC antibody and Dr. Kazuhiro Aoki (Tokyo Medical and Dental University) for technical assistance in the measurement of BMD.

REFERENCES

1. Murakami, M., and Kudo, I. (2004) *Prog. Lipid Res.* **43**, 3–35
2. Sugimoto, Y., Narumiya, S., and Ichikawa, A. (2000) *Prog. Lipid Res.* **39**, 289–314
3. Murakami, M., Nakatani, Y., Tanioka, T., and Kudo, I. (2002) *Prostaglandins Other Lipid Mediat.* **68–69**, 383–399
4. Murakami, M., Naraba, H., Tanioka, T., Semmyo, N., Nakatani, Y., Kojima, F., Ikeda, T., Fueki, M., Ueno, A., Oh-Ishi, S., and Kudo, I. (2000) *J. Biol. Chem.* **275**, 32783–32792
5. Jakobsson, P. J., Thoren, S., Morgenstern, R., and Samuelsson, B. (1999) *Proc. Natl. Acad. Sci. U. S. A.* **96**, 7220–7225
6. Mancini, J. A., Blood, K., Guay, J., Gordon, R., Claveau, D., Chan, C. C., and Riendeau, D. (2001) *J. Biol. Chem.* **276**, 4469–4475
7. Stichtenoth, D. O., Thoren, S., Bian, H., Peters-Golden, M., Jakobsson, P. J., and Crofford, L. J. (2001) *J. Immunol.* **167**, 469–474
8. Yamagata, K., Matsumura, K., Inoue, W., Shiraki, T., Suzuki, K., Yasuda, S., Sugiura, H., Cao, C., Watanabe, Y., and Kobayashi, S. (2001) *J. Neurosci.* **21**, 2669–2677
9. Filion, F., Bouchard, N., Goff, A. K., Lussier, J. G., and Sirois, J. (2001) *J. Biol. Chem.* **276**, 34323–34330
10. Claveau, D., Sirinyan, M., Guay, J., Gordon, R., Chan, C. C., Bureau, Y., Riendeau, D., and Mancini, J. A. (2003) *J. Immunol.* **70**, 4738–4744
11. Thoren, S., Weinander, R., Saha, S., Jegerschold, C., Pettersson, P. L., Samuelsson, B., Hebert, H., Hamberg, M., Morgenstern, R., and Jakobsson, P. J. (2003) *J. Biol. Chem.* **278**, 22199–22209
12. Kamei, D., Murakami, M., Nakatani, Y., Ishikawa, Y., Ishii, T., and Kudo, I. (2003) *J. Biol. Chem.* **278**, 19396–19405
13. Han, R., Tsui, S., and Smith, T.J. (2002) *J. Biol. Chem.* **277**, 16355–16364
14. Naraba, H., Yokoyama, C., Tago, N., Murakami, M., Kudo, I., Fueki, M., Oh-Ishi, S., and Tanabe, T. (2002) *J. Biol. Chem.* **277**, 28601–28608
15. Tanikawa, N., Ohmiya, Y., Ohkubo, H., Hashimoto, K., Kangawa, K., Kojima, M., Ito, S., and Watanabe, K. (2002) *Biochem. Biophys. Res. Commun.* **291**, 884–889
16. Murakami, M., Nakashima, K., Kamei, D., Masuda, S., Ishikawa, Y., Ishii, T., Ohmiya, Y., Watanabe, K., and Kudo, I. (2003) *J. Biol. Chem.* **278**, 37937–37947
17. Tanioka, T., Nakatani, Y., Semmyo, N., Murakami, M., and Kudo, I. (2000) *J. Biol. Chem.* **275**, 32775–32782
18. Tanioka, T., Nakatani, Y., Kobayashi, T., Tsujimoto, M., Oh-ishi, S., Murakami, M., and Kudo, I. (2003) *Biochem. Biophys. Res. Commun.* **303**, 1018–1023
19. Beuckmann, C. T., Fujimori, K., Urade, Y., and Hayaishi, O. (2000) *Neurochem. Res.* **25**, 733–738
20. Uematsu, S., Matsumoto, M., Takeda, K., and Akira, S. (2002) *J. Immunol.* **168**, 5811–5816
21. Tanaka, S., Nemoto, K., Yamamura, E., and Ichikawa, A. (1998) *J. Biol. Chem.* **273**, 8177–8182
22. Naraba, H., Murakami, M., Matsumoto, H., Shimbara, S., Ueno, A., Kudo, I., and Oh-ishi, S. (1998) *J. Immunol.* **160**, 2974–2982
23. Matsumoto, H., Naraba, H., Ueno, A., Fujiyoshi, T., Murakami, M., Kudo, I., and Oh-ishi, S. (1998) *Eur. J. Pharmacol.* **352**, 47–52
24. Ueno, A., Matsumoto, H., Naraba, H., Ikeda, Y., Ushikubi, F., Matsuoka, T., Narumiya, S., Sugimoto, Y., Ichikawa, A., and Oh-ishi, S. (2001) *Biochem. Pharmacol.* **62**, 157–160
25. Ghosh, A. K., Hirasawa, N., Ohtsu, H., Watanabe, T., and Ohuchi, K. (2002) *J. Exp. Med.* **195**, 973–982
26. Terato, K., Hasty, K. A., Reife, R. A., Cremer, M. A., Kang, A. H., and Stuart, J. M. (1992) *J. Immunol.* **148**, 2103–2108
27. Terato, K., Harper, D. S., Griffiths, M. M., Hasty, D. L., Ye, X. J., Cremer, M. A., and Seyer, J. M. (1995) *Autoimmunity* **22**, 137–147
28. Azuma, Y., Oue, Y., Kanatani, H., Ohta, T., Kiyoki, M., and Komoriya, K. (1998) *J. Pharmacol. Exp. Ther.* **286**, 128–135
29. Guan, Y., Zhang, Y., Schneider, A., Riendeau, D., Mancini, J. A., Davis, L., Kombhoff, M., Breyer, R. M., and Breyer, M. D. (2001) *Am. J. Physiol.* **281**, F1173–F1177
30. Murata, T., Ushikubi, F., Matsuoka, T., Hirata, M., Yamasaki, A., Sugimoto, Y., Ichikawa, A., Aze, Y., Tanaka, T., Yoshida, N., Ueno, A., Oh-ishi, S., and Narumiya, S. (1997) *Nature* **388**, 678–682
31. Stock, J. L., Shinjo, K., Burkhardt, J., Roach, M., Taniguchi, K., Ishikawa, T., Kim, H. S., Flannery, P. J., Coffman, T. M., McNeish, J. D., and Audoly, L. P. (2001) *J. Clin. Invest.* **107**, 325–331
32. Ballou, L. R., Botting, R. M., Goorha, S., Zhang, J., and Vane, J. R. (2000) *Proc. Natl. Acad. Sci. U. S. A.* **97**, 10272–10276
33. Schuligoi, R., Ulcar, R., Peskar, B. A., and Amann, R. (2003) *Neuroscience* **116**, 1043–1052
34. Ueno, N., Murakami, M., Tanioka, T., Fujimori, K., Urade, Y., and Kudo, I. (2001) *J. Biol. Chem.* **276**, 34918–34927
35. Nakashima, K., Ueno, N., Kamei, D., Tanioka, T., Nakatani, Y., Murakami, M., and Kudo, I. (2003) *Biochim. Biophys. Acta* **1633**, 96–105
36. Myers, L. K., Kang, A. H., Postlethwaite, A. E., Rosloniec, E. F., Morham, S. G., Shlopov, B. V., Goorha, S., and Ballou, L. R. (2000) *Arthritis Rheum.* **43**, 2687–2693
37. Matsumoto, A. K., Melian, A., Mandel, D. R., McIlwain, H. H., Borenstein, D., Zhao, P. L., Lines, C. R., Gertz, B. J., and Curtis, S. (2002) *J. Rheumatol.* **29**, 1623–1630
38. Portanova, J. P., Zhang, Y., Anderson, G. D., Hauser, S. D., Masferrer, J. L., Seibert, K., Gregory, S. A., and Isakson, P. C. (1996) *J. Exp. Med.* **184**, 883–891
39. Vane, J. R., and Botting, R. M. (1995) *Inflamm. Res.* **44**, 1–10
40. Mehindate, K., al-Daccak, R., Dayer, J. M., Kennedy, B. P., Kris, C., Borgeat, P., Poubelle, P. E., and Mourad, W. (1995) *J. Immunol.* **155**, 3570–3577
41. Ben-Av, P., Crofford, L. J., Wilder, R. L., and Hla, T. (1995) *FEBS Lett.* **372**, 83–87
42. Bensen, W., Weaver, A., Espinoza, L., Zhao, W. W., Riley, W., Paperiello, B., and Recker, D. P. (2002) *Rheumatology (Oxf.)* **41**, 1008–1016
43. Wooley, P. H., Luthra, H. S., Stuart, J. M., and David, C. S. (1981) *J. Exp. Med.* **154**, 688–700
44. Trebino, C. E., Stock, J. L., Gibbons, C. P., Naiman, B. M., Wachtmann, T. S., Umland, J. P., Pandher, K., Lapointe, J. M., Saha, S., Roach, M. L., Carter, D., Thomas, N. A., Durtschi, B. A., McNeish, J. D., Hambor, J. E., Jakobsson, P. J., Carty, T. J., Perez, J. R., and Audoly, L. P. (2003) *Proc. Natl. Acad. Sci. U. S. A.* **100**, 9044–9049
45. Ghosh, A. K., Hirasawa, N., Niki, H., and Ohuchi, K. (2000) *J. Pharmacol. Exp. Ther.* **295**, 802–809
46. Sonoshita, M., Takaku, K., Sasaki, N., Sugimoto, Y., Ushikubi, F., Narumiya, S., Oshima, M., and Taketo, M. M. (2001) *Nat. Med.* **7**, 1048–1051
47. Amano, H., Hayashi, I., Endo, H., Kitasato, H., Yamashina, S., Maruyama, T., Kobayashi, M., Satoh, K., Narita, M., Sugimoto, Y., Murata, T., Yoshimura, H., Narumiya, S., and Majima, M. (2003) *J. Exp. Med.* **197**, 221–232
48. Siegle, I., Klein, T., Backman, J. T., Saal, J. G., Nusing, R. M., and Fritz, P. (1998) *Arthritis Rheum.* **41**, 122–129
49. Hegen, M., Sun, L., Uozumi, N., Kume, K., Goad, M. E., Nickerson-Nutter, C. L., Shimizu, T., and Clark, J. D. (2003) *J. Exp. Med.* **197**, 1297–1302
50. McCoy, J. M., Wicks, J. R., and Audoly, L. P. (2002) *J. Clin. Invest.* **110**, 651–658
51. Saegusa, M., Murakami, M., Nakatani, Y., Yamakawa, K., Katagiri, M., Matsuda, K., Nakamura, K., Kudo, I., and Kawaguchi, H. (2003) *J. Cell. Physiol.* **197**, 348–356
52. Li, J., Sarosi, I., Yan, X. Q., Morony, S., Capparelli, C., Tan, H. L., McCabe, S., Elliott, R., Scully, S., Van, G., Kaufman, S., Juan, S. C., Sun, Y., Tarpley, J., Martin, L., Christensen, K., McCabe, J., Kostenuik, P., Hsu, H., Fletcher, F., Dunstan, C. R., Lacey, D. L., and Boyle, W. J. (2000) *Proc. Natl. Acad. Sci. U. S. A.* **97**, 1566–1571
53. Udagawa, N., Kotake, S., Kamatani, N., Takahashi, N., and Suda, T. (2002) *Arthritis Res.* **4**, 281–289
54. Manabe, N., Oda, H., Nakamura, K., Kuga, Y., Uchida, S., and Kawaguchi, H. (1999) *Rheumatology (Oxf.)* **38**, 714–720
55. Chikazu, D., Katagiri, M., Ogasawara, T., Ogata, N., Shimoaka, T., Takato, T., Nakamura, K., and Kawaguchi, H. (2001) *J. Bone Miner. Res.* **16**, 2074–2081
56. Suda, T., Takahashi, N., Udagawa, N., Jimi, E., Gillespie, M. T., and Martin, T. J. (1999) *Endocr. Rev.* **20**, 345–357
57. Lader, C. S., and Flanagan, A. M. (1998) *Endocrinology* **139**, 3157–3164
58. Suda, K., Udagawa, N., Sato, N., Takami, M., Itoh, K., Woo, J. T., Takahashi, N., and Nagai, K. (2004) *J. Immunol.* **172**, 2504–2510
59. Wani, M. R., Fuller, K., Kim, N. S., Choi, Y., and Chambers, T. (1999) *Endocrinology* **140**, 1927–1935
60. Li, X., Okada, Y., Pilbeam, C. C., Lorenzo, J. A., Kennedy, C. R., Breyer, R. M., and Raisz, L. G. (2000) *Endocrinology* **141**, 2054–2061
61. Rocca, B., Spain, L.M., Pure, E., Langenbach, R., Patrono, C., and FitzGerald, G. A. (1999) *J. Clin. Invest.* **103**, 1469–1477
62. Lorenz, M., Slaughter, H. S., Wescott, D. M., Carter, S. I., Schnyder, B., Dinchuk, J. E., and Car, B. D. (1999) *Exp. Hematol.* **27**, 1494–1502
63. Desplat, V., Besse, A., Denizot, Y., and Praloran, V. (2000) *Exp. Hematol.* **28**, 741–742

64. Besse, A., Trimoreau, F., Faucher, J. L., Praloran, V., and Denizot, Y. (1999) *Biochim. Biophys. Acta* **1450**, 444–451
65. Soruri, A., Riggert, J., Schlott, T., Kiafard, Z., Dettmer, C., and Zwirner, J. (2003) *J. Immunol.* **171**, 2631–2636
66. Scandella, E., Men, Y., Gillenssen, S., Forster, R., and Groettrup, M. (2002) *Blood* **100**, 1354–1361
67. Takeda, H., Sonoshita, M., Oshima, H., Sugihara, K., Chulada, P. C., Langenbach, R., Oshima, M., and Taketo, M. M. (2003) *Cancer Res.* **63**, 4872–4877
68. Engblom, D., Saha, S., Engstrom, L., Westman, M., Audoly, L. P., Jakobsson, P. J., and Blomqvist, A. (2003) *Nat. Neurosci.* **6**, 1137–1138
69. Kabashima, K., Saji, T., Murata, T., Nagamachi, M., Matsuoka, T., Segi, E., Tsuboi, K., Sugimoto, Y., Kobayashi, T., Miyachi, Y., Ichikawa, A., and Narumiya, S. (2002) *J. Clin. Invest.* **109**, 883–893
70. Morteau, O., Morham, S. G., Sellon, R., Dieleman, L. A., Langenbach, R., Smithies, O., and Sartor, R. B. (2000) *J. Clin. Invest.* **105**, 469–478
71. Bonner, J. C., Rice, A. B., Ingram, J. L., Moomaw, C. R., Nyska, A., Bradbury, A., Sessoms, A. R., Chulada, P. C., Morgan, D. L., Zeldin, D. C., and Langenbach, R. (2002) *Am. J. Pathol.* **161**, 459–470
72. Norwood, V. F., Morham, S. G., and Smithies, O. (2000) *Kidney Int.* **58**, 2291–2300
73. Loftin, C. D., Trivedi, D. B., Tiano, H. F., Clark, J. A., Lee, C. A., Epstein, J. A., Morham, S. G., Breyer, M. D., Nguyen, M., Hawkins, B. M., Goulet, J. L., Smithies, O., Koller, B. H., and Langenbach, R. (2001) *Proc. Natl. Acad. Sci. U. S. A.* **98**, 1059–1064
74. Segi, E., Sugimoto, Y., Yamasaki, A., Aze, Y., Oida, H., Nishimura, T., Murata, T., Matsuoka, T., Ushikubi, F., Hirose, M., Tanaka, T., Yoshida, N., Narumiya, S., and Ichikawa, A. (1998) *Biochem. Biophys. Res. Commun.* **246**, 7–12
75. Hizaki, H., Segi, E., Sugimoto, Y., Hirose, M., Saji, T., Ushikubi, F., Matsuoka, T., Noda, Y., Tanaka, T., Yoshida, N., Narumiya, S., and Ichikawa, A. (1999) *Proc. Natl. Acad. Sci. U. S. A.* **96**, 10501–10596

Cyclic GMP-dependent protein kinase II is a molecular switch from proliferation to hypertrophic differentiation of chondrocytes

Hirotaka Chikuda,[1] Fumitaka Kugimiya,[1] Kazuto Hoshi,[1] Toshiyuki Ikeda,[1] Toru Ogasawara,[1] Takashi Shimoaka,[1] Hirotaka Kawano,[1] Satoru Kamekura,[1] Atsuko Tsuchida,[2] Norihide Yokoi,[2] Kozo Nakamura,[1] Kajuro Komeda,[2] Ung-il Chung,[1] and Hiroshi Kawaguchi[1,3]

[1]Department of Sensory and Motor System Medicine, Faculty of Medicine, University of Tokyo, Bunkyo, Tokyo 113-8655, Japan; [2]Division of Laboratory Animal Science, Animal Research Center, Tokyo Medical University, Shinjuku, Tokyo 160-8402, Japan

The Komeda miniature rat Ishikawa (KMI) is a naturally occurring mutant caused by an autosomal recessive mutation *mri*, which exhibits longitudinal growth retardation. Here we identified the *mri* mutation as a deletion in the rat gene encoding cGMP-dependent protein kinase type II (cGKII). KMIs showed an expanded growth plate and impaired bone healing with abnormal accumulation of postmitotic but nonhypertrophic chondrocytes. Ex vivo culture of KMI chondrocytes reproduced the differentiation impairment, which was restored by introducing the adenovirus-mediated *cGKII* gene. The expression of Sox9, an inhibitory regulator of hypertrophic differentiation, persisted in the nuclei of postmitotic chondrocytes of the KMI growth plate. Transfection experiments in culture systems revealed that cGKII attenuated the Sox9 functions to induce the chondrogenic differentiation and to inhibit the hypertrophic differentiation of chondrocytes. This attenuation of Sox9 was due to the cGKII inhibition of nuclear entry of Sox9. The impaired differentiation of cultured KMI chondrocytes was restored by the silencing of Sox9 through RNA interference. Hence, the present study for the first time shed light on a novel role of cGKII as a molecular switch, coupling the cessation of proliferation and the start of hypertrophic differentiation of chondrocytes through attenuation of Sox9 function.

[*Keywords*: KMI; cGKII; Sox9; chondrocyte; hypertrophy; endochondral ossification]

Received May 20, 2004; revised version accepted August 4, 2004.

Skeletal growth is determined mainly by the process of endochondral ossification in the cartilaginous growth plate, which consists of the resting, proliferative, and hypertrophic zones of chondrocytes, typically in orderly columnar arrays. In this process, chondrocytes that arise from mesenchymal cells undergo proliferation, terminal differentiation into hypertrophic cells, and synthesis of the cartilage matrix, which finally calcifies and is replaced by bone (Kronenberg 2003). The start of hypertrophic differentiation occurs concurrently with the cessation of chondrocyte proliferation. To date, several molecular signalings have been implicated in the switching between proliferation and terminal differentiation in other cell types (Sorrentino et al. 1990; Umek et al. 1991; Tao and Umek 2000); however, the molecular mechanism that couples the cessation of proliferation and the start of hypertrophic differentiation of chondrocytes remains an enigma.

The Komeda miniature rat Ishikawa (KMI), which was discovered in a closed colony of Wistar rats and was established as a segregating inbred, is a naturally occurring dwarf mutant caused by an autosomal recessive mutation *mri* (Serizawa 1993). Homozygous mutants (*mri*/*mri*) were born and grew normally until 3–4 wk of age, when they gradually started to develop longitudinal growth retardation without other organ abnormalities. In the present study we identified the *mri* mutation as a deletion in the rat gene encoding cGMP-dependent protein kinase type II (cGKII) by a positional candidate cloning strategy. cGKII is a membrane-bound kinase which is activated by intracellular cGMP, and is known to be expressed abundantly in the intestinal mucosa, kidney, lung, brain, and cartilage (Ruth 1999; Hofmann et al. 2000). This study further investigated the cellular and molecular mechanisms underlying the impairment of endochondral ossification by the cGKII deficiency.

[3]Corresponding author.
E-MAIL kawaguchi-ort@h.u-tokyo.ac.jp; FAX 81-3-3818-4082.
Article and publication are at http://www.genesdev.org/cgi/doi/10.1101/gad.1224204.

Results

*Longitudinal growth retardation in KMI (*mri/mri*)*

KMIs developed dwarfism with short limbs and trunk compared to the wild-type littermates (Fig. 1A). Growth curves indicated that KMIs started to show the axial growth retardation postnatally at 4 wk of age, although there was no difference between wild-type and heterozygote (*+/mri*) rats in either sex, confirming an autosomal recessive inheritance (Fig. 1B). The trunk of the KMIs was about 30% shorter than those of wild-type and *+/mri* littermates at 10 wk of age. Skeletal X-ray analysis at this age revealed no appreciable changes between wild type and KMI in the width of calvarium, which is formed through intramembranous ossification; however, the longitudinal lengths of femora, tibiae, and vertebrae, all of which are formed through endochondral ossification, were 20%–30% shorter in KMI than in wild type (Fig. 1C,D). In the long bones of KMI, the height of the epiphyseal growth plate was greater than that in wild type, indicating that the growth retardation in KMI resulted from the impairment of endochondral ossification in the growth plate.

Positional cloning of the mri *mutation*

We first genotyped simple sequence length polymorphism (SSLP) markers throughout the rat genome on the backcross progeny and detected putative linkage at the *D14Rat6* marker on rat chromosone 14. Further genetic mapping localized the *mri* locus to a 1.2-cM interval on rat chromosome 14 flanked by markers *D14Rat5* and *D14Rat80*. Comparative mapping analysis revealed that the region was orthologous to the regions on mouse chromosome 5 and human chromosome 4, in which several candidate genes including *Bmp3* and *cGKII* (also known as *Prkg2*) were identified (Fig. 2A). Although the *Bmp3* gene encoding a bone morphogenetic protein (BMP) first drew our attention, our studies revealed this gene unlikely to be causative of the KMI phenotype. The expression of the *Bmp3* gene was not different between wild type and KMI, and the sequencing analysis showed only a few silent variants (data not shown). Furthermore, the *Bmp3* null mice are reported to exhibit normal body size but increased bone density (Daluiski et al. 2001), which is different from the KMI phenotypes.

We then performed an RT–PCR analysis of the *cGKII* gene, and found that the cGKII transcript from the brain of the KMI mutant was shorter than that from wild type (Fig. 2B). Sequencing analysis disclosed that exon 3 of the *cGKII* gene was directly spliced onto exon 6 (Fig. 2C). This 220-bp deletion spanning exons 4 and 5 resulted in a frame shift and a premature stop codon, predicting a truncated product that lacks the entire kinase domain (Fig. 2D). We further carried out inter-exon PCR between exons 3 and 6 of the genomic DNA, and found an ~5-kb

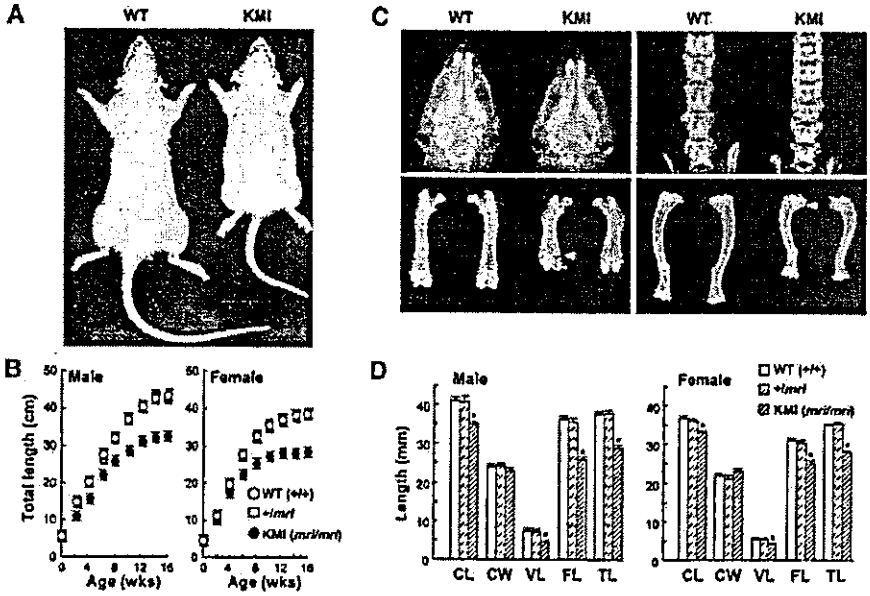

Figure 1. Longitudinal growth retardation in KMI (*mri/mri*). (*A*) Gross appearance of wild-type (WT) and KMI littermates at 10 wk of age. (*B*) Growth curves of wild-type (WT; +/+), heterozygote (*+/mri*), and homozygote (KMI, *mri/mri*) rats determined by the total axial length (from nose to tail end). The symbols of *+/mri* are behind those of wild-type rats. Data are expressed as means (symbols) ± S.E.M. (error bars) for 12 rats/group. (*C*) Plain X-ray images of heads (*top left*), lumbar vertebrae (*top right*), femora (*bottom left*), and tibiae (*bottom right*) of wild-type (WT) and KMI littermates at 10 wk. Arrowheads indicate the expanded growth plates in KMI. (*D*) Bone lengths of wild type (WT), *+/mri*, and KMI at 10 wk. (CL) Naso-occipital length of the calvarium; (CW) maximal interparietal distance of the calvarium; (VL) fifth lumbar vertebral length; (FL) femoral length; (TL) tibial length. Data are means (bars) ± S.E.M. (error bars) for 12 rats/group. (*) $P < 0.05$ vs. wild type.

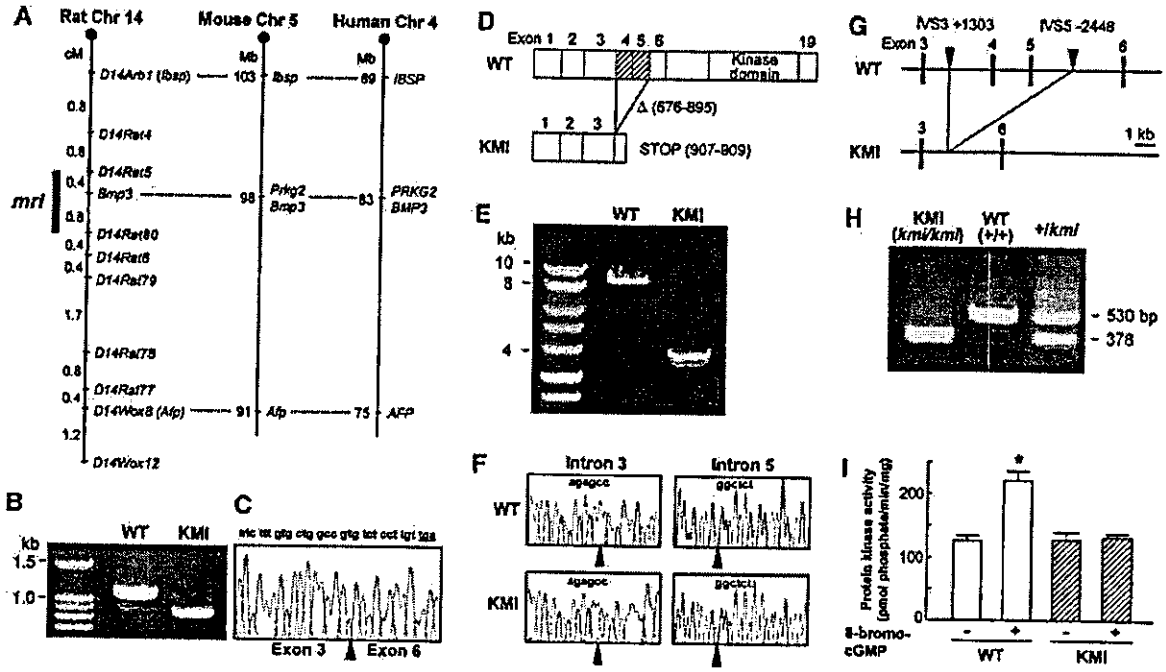

Figure 2. Identification of the *mri* mutation. (*A*) Comparative mapping of the *mri* region in the rat, mouse, and human choromosomes. The *mri* locus, which was mapped to a 1.2-cM interval between markers *D14rat5* and *D14rat80*, is shown as a bold line. (*B*) RT–PCR products of the rat cGKII from the brains of wild-type (WT) and KMI littermates. (*C*) Sequence analysis of transcript of the *cGKII* gene from the KMI mutant. Exon 3 is directly spliced onto exon 6, with the boundary indicated by the arrowhead. The frame shift causes amino acid substitutions and a premature stop codon. (*D*) Schematic representation of the prematurely truncated cGKII protein in the KMI mutant. Nucleotide sequence analyses of the cDNA identified a 220-bp deletion (676–895) corresponding to exons 4 and 5. (*E*) Interexon PCR between exons 3 and 6 using the genomic DNA from wild type (WT) and KMI indicated an ~5-kb deletion in the KMI. (*F*) Sequence analyses of genomic DNA of wild type (WT) and KMI identified breakpoints in introns 3 and 5 (arrowheads). A common sequence, "AGAGCC", was found at the two breakpoints. (*G*) Schematic representation of the *mri* mutation as an ~5-kb deletion in the *cGKII* gene. Sequence analyses disclosed the deletion from IVS3+1303 to IVS5–2448 in KMI. (*H*) Genotyping of KMI (*mri/mri*), wild-type (WT; +/+), and +/*mri* rats. A longer amplicon (530 bp) was amplified from wild-type allele, and a shorter amplicon (378 bp) from the mutated allele. (*I*) Lack of cGMP-dependent protein kinase activity of the KMI brain extract determined by the in vitro kinase assay in the presence and absence of 8-bromo-cGMP. Data are means (bars) ± S.E.M. (error bars) of six samples/group. (*) $P < 0.01$, significant effect of 8-bromo-cGMP.

deletion in the *cGKII* gene of KMI (Fig. 2E). Sequencing analysis identified the breakpoints in introns 3 and 5, both of which had a common sequence, "AGAGCC" (Fig. 2F), creating a deletion from intervening sequence (IVS)3+1303 to IVS5–2448 (Fig. 2G). To confirm that this deletion in the *cGKII* gene was responsible for the KMI phenotype, we designed PCR primers to detect this genomic deletion, and found complete cosegregation of the genotypes KMI (*mri/mri*), wild type (+/+), and +/*mri* with the phenotypes (Fig. 2H). To test whether the *mri* mutation in the *cGKII* gene resulted in loss of its function, tissue extract from brain that is known to express high levels of cGKII was assayed for the kinase activity. The in vitro kinase assay revealed that the wild-type extract showed a significant increase in the kinase activity by the stimulation with the cGMP analog 8-bromo-cGMP; however, the increase was not observed in the KMI extract (Fig. 2I). Taken together, these results strongly suggested that the deletion in the *cGKII* gene resulted in loss of its function and caused dwarfism in KMI.

Abnormal endochondral ossification in the growth plate and the fracture callus of KMI

We first investigated the expression pattern of cGKII in the proximal growth plates of the wild-type and KMI tibiae at 10 wk of age. Immunohistochemical analysis of the wild-type growth plate revealed that cGKII was expressed predominantly in the late proliferative and prehypertrophic chondrocytes, preceding the start of hypertrophic differentiation; however, no immunoreactivity for cGKII was observed in the KMI growth plate (Fig. 3A, α-cGKII).

To elucidate the cellular mechanisms underlying the dwarfism due to the cGKII dysfunction in KMI, we performed histological analyses of the growth plates. At birth, growth plates showed no discernible difference between wild type and KMI (Fig. 3A, HE, E18.5). Pathological changes gradually became evident postnatally after 4–5 wk of age, and at 10 wk the height of the KMI growth plate was about 2.5-fold greater than that of wild type

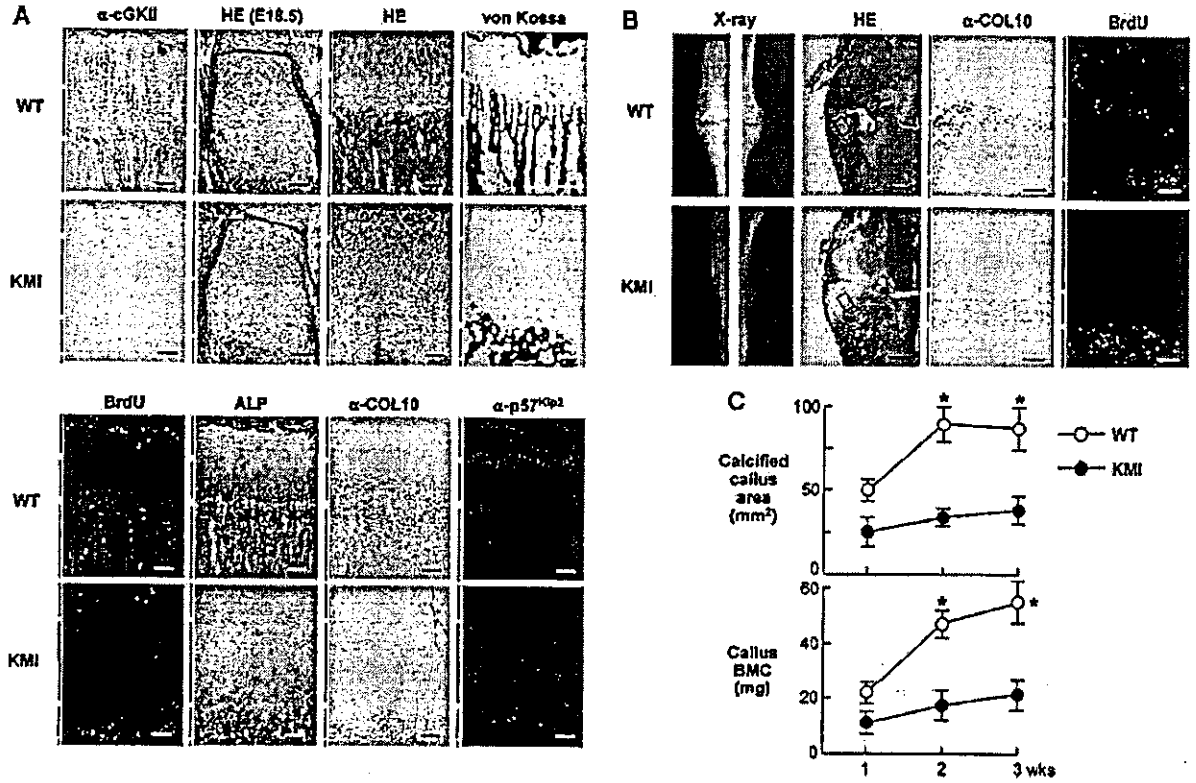

Figure 3. Comparison of endochondral ossification in the growth plate (*A*) and the bone fracture callus (*B,C*) between wild type (WT) and KMI. Blue, red, and green bars indicate layers of proliferative zone, hypertrophic (including prehypertrophic) zone, and primary spongiosa, respectively. Black bar indictates the abnormal intermediate zone that is seen only in KMI. (*A*) Histological findings of the proximal growth plates in wild-type (WT) and KMI tibiae at 10 wk of age unless otherwise described. (*Upper* panel) Immunohistochemical staining with an anti-cGKII antibody (α-cGKII), hematoxylin-eosin staining of the humeral growth plates of fetal rats (HE, E18.5), HE staining (HE), and von Kossa staining (von Kossa). (*Lower* panel) BrdU labeling (BrdU), alkaline phosphatase staining (ALP), immunohistochemical stainings with anti-type X collagen (α-COL10), and anti-p57^{Kip2} (α-p57^{Kip2}) antibodies. Bars, 50 μm. (*B*) Radiological and histological findings of the fracture callus 2 wk after the surgery. After exposing the right tibiae of 10-week-old rats, a transverse osteotomy was performed at the midshaft with a bone saw and was stabilized with an intramedullary nail. Plain X-ray images (X-ray), HE staining (HE; *inset* boxes indicate the regions of the *right* two figures), immunohistochemical staining with an anti-type X collagen antibody (α-COL10), and BrdU labeling (BrdU). Bars: HE, 500 μm; *right* two figures, 50 μm. (*C*) Time course of the calcified area and the bone mineral content (BMC) of the callus at the fracture site measured by a single energy X-ray absorptiometry. Data are mean (symbols) ± S.E.M. (error bars) of eight rats/genotype. (*) $P < 0.01$ vs. wild type.

(665 ± 47 μm vs. 255 ± 34 μm, mean ± S.E.M., $n = 8$, respectively), although the columnar structure was relatively preserved (Fig. 3A, HE). This increase was due to an intermediate layer of accumulated abnormal chondrocytes in the KMI growth plate (Fig. 3A, HE, black bar). Although the cell size of chondrocytes in the KMI hypertrophic zone seemed somewhat smaller than that in wild type, matrix mineralization determined by von Kossa staining appeared normal in KMI (Fig. 3A, von Kossa).

To further characterize the abnormal chondrocytes in the intermediate layer of the KMI growth plate, we examined cellular proliferation by the the uptake of BrdU. In wild type, chondrocytes in the proliferating zone and bone marrow cells in the primary spongiosa were actively proliferating as detected by the BrdU uptake (Fig. 3A, BrdU). In KMI, the number of BrdU-positive cells was slightly decreased in the proliferating zone, and more importantly, no uptake was observed in the intermediate layer, suggesting that these abnormal chondrocytes were postmitotic. We next examined the distributions of alkaline phosphatase (ALP) and type X collagen (COL10) as markers of prehypertrophic and hypertrophic chondrocytes, respectively. Histochemical analyses of the wild-type growth plate revealed that these markers were expressed immediately after the BrdU uptake had disappeared, confirming the coupling of the cessation of proliferation and the start of hypertrophic differentiation (Fig. 3A, ALP and α-COL10). In the KMI growth plate, however, the intermediate layer was stained by neither of the markers, indicating that these abnormal chondrocytes had not started hypertrophic differentiation. In addition, expression of p57^{Kip2}, a key regulator of cell-cycle arrest and differentiation of chondrocytes (Yan et al.